Doctoral Thesis

Study on Electrolysis-based Tritium in Water Real-Time Continuous Monitoring System

Jun Woo Bae

Department of Nuclear Engineering

Ulsan National Institute of Science and Technology

2021

Study on Electrolysis-based Tritium in Water Real-Time Continuous Monitoring System

Jun Woo Bae

Department of Nuclear Engineering

Ulsan National Institute of Science and Technology

Study on Electrolysis-based Tritium in Water Real-Time Continuous Monitoring System

A thesis/dissertation submitted to
Ulsan National Institute of Science and Technology
in partial fulfillment of the
requirements for the degree of
Doctor of Philosophy

Jun Woo Bae

12/09/2020 of submission

Approved by

Advisor
Hee Reyoung Kim

Study on Electrolysis-based Tritium in Water Real-Time Continuous Monitoring System

Jun Woo Bae

This certifies that the thesis/dissertation of Jun Woo Bae is approved.

12/09/2020

Advisor: Hee Reyoung Kim

Seung Jun Lee

Jaeyoung Park

Pil Woo Heo

Sangbum Hong

Abstract

Monitoring of tritium in water is important in the aspect of radiological protection. The tritium only emits beta ray with extremely low energy, it is categorized by hard-to-detect radionuclide. Because of its low energy, self-absorption effect is very high and detection efficiency of direct measurement of tritium is very low. Therefore, the tritium-in-water monitoring system was developed including gasification using electrolysis to reduce the self-absorption effect and specialized design of detection chamber to increase the detection efficiency. The concentration of the tritiated gas generated by electrolysis is determined by fractionation factor. The fractionation factor was estimated, and its temperature dependence was quantified. The lowest fractionation factor was obtained as 3.24 ± 0.14 at temperature of 90 ℃. A novel design of detection chamber which was specialized to detect the low energy beta ray was proposed. In the detection chamber, plastic scintillators were placed with narrow gap to reduce worthless space and increase the detection efficiency. The performance of the detection including detection efficiency and MDA for the developed chamber was evaluated using MCNP6 simulation. The highest detection efficiency was close to 100% and detection efficiency of 53.7% was shown in 32-channel chamber. The lowest MDA was shown at the chamber when 0.5 mm of plastic scintillator was placed with 48-channel and its value was 29.9 kBq/m^3 with the counting time of 30 s which was lower than any other comparing studies. Because of the practical processing limitations of the acrylic which was selected as a supporting structure of plastic scintillators, a 12-channel detection chamber using 1 mm plastic scintillator was manufactured. Signal processing parameters were optimized, the maximum detection efficiency was estimated by 43.0 ± 4.32%. In the integrated system, detection efficiency was estimated by 18.8±2.4 %, and MDA for the liquid tritiated water was estimated by 5 kBq/L with measurement time of 600 min.

Contents

Figure Captions

Table Captions

Nomenclature

Abbreviations

CPS	Counts Per Second
FOM	Figure of Merit
FWHM	Full Width Half Maximum
LDL	Lower Discrimination Level
LSC	Liquid Scintillation Counter
MCA	Multi-Channel Analyzer
MCNP	Monte Caro N-Particle
MDA	Minimum Detectable Activity
P-10	Fill gas for proportional counters of ionizing radiation, consisting of 90% argon and 10% methane
PEM	Polymer Electrolyte Membrane
PMMA	Poly-methyl Methacrylate
ROI	Range of Interest
SCA	Single-Channel Analyzer
TAC	Time to Amplitude Converter

Symbols (in order of appearance)

R_β	Range of the beta ray
E_β	Energy of the beta ray
β	Fractionation factor
E	Enrichment factor
T_0	Initial concentration of the tritium in water
T	Final concentration of the tritium in water
V_0	Initial volume of the tritiated water sample
V	Final volume of the tritiated water sample
T_{gas}	Tritium concentration in an electrolyzed gaseous sample
T_{liquid}	Tritium concentration in liquid sample to be electrolyzed
κ	Hydrogen volume correction factor
ε_{area}	Specific detection efficiency
CR	Net counting rate
A	Surface area of plastic scintillator
M	Volume of detection chamber
t	Measurement time
ε	Detection Efficiency
Cs	Counts for present (sample) measurement
C_B	Background counts
T_S	Sample measurement time
T_B	Background measurement time
MDA_{gas}	MDA in case of gaseous tritium detection
MDA_{liquid}	MDA applied for tritium in water detection

Chapter I. Introduction

1.1 Research Background

Tritium is one of the most concerning radionuclides because it is easy to intake through drinking water, food, or tritiated water vapor. Tritium exists as form of tissue-free water tritium or organically bound tritium [1]. The tissue-free water tritium is easily removed during metabolism. However, because the organically bound tritium becomes a constituent of the body, it cannot be removed easily during metabolism, which may lead to long-term exposure [2]. The tritium in the environment is generated by both natural and artificial ways. Because of natural production by interaction of a cosmic ray and ^{14}N in atmosphere, a certain amount of tritium concentration is maintained worldwide [3]. Until 1963, as the nuclear test was widely conducted, the concentration of tritium increased, but it decreased sharply thereafter [4]. Subsequent main production of tritium is release during operation of nuclear power plants and emissions after nuclear accidents. In particular, pressurized heavy water reactors release more tritium due to the use of deuterium [5, 6], and tritium release after Fukushima Daiichi accident [7] is concerning. Based on these cases, radioactivity monitoring of tritium-in-water is important in the aspect of radiation protection and reduction of public fear against to the radioactivity.

Tritium is a hard-to-detect radionuclide because it is pure-beta emitter which means that no following gamma ray emission after decay and its energy of emitting beta ray is extremely low with maximum energy of 18.6 keV [8]. A conventional method for detection of tritium in water is sampling from field, distillation or combustion in laboratory and measurement of the beta ray using liquid scintillation counter (LSC) [9, 10]. The LSC is suitable for tritiated detection of an environmental sample because of its high efficiency for tritium measurement and low minimum detectable activity (MDA). However, using a liquid scintillator to analyze large amount of tritiated water sample such as continuous monitoring is not recommended because toxicity of the liquid scintillator is very high [11], resulting in generation of large amount of organic waste. Though the conventional method has merit on precise analysis for very-low level of tritium activity, but it is not suitable for continuous monitoring for large

amount of water sample. Moreover, because it is not real-time monitoring, it be a monitoring method of preparing for accidents such as leakage of cooling water from a nuclear power plant [12].

1.2 Literature Study

1) Commercial Liquid-state tritium monitors

There are commercial detector models for tritium measurement in the water samples, such as the LIQ-X series and NEXGEN series (Technical associates). The detection limit of LIQ-X series is 370 kBq/L for a measurement time of 2 hours. The method of operation for the LIQ-X model is automatic pumping of water samples for direct measurement using liquid scintillator. However, it has a relatively high detection limit and use of liquid scintillator is not desirable for continuous monitoring of water. For low level of tritium monitoring, NEXGEN model is preferred which has detection limit of 14.8 kBq/L in 4 h. In this model, tritium is detected by flowing water through the crushed scintillator bed. In this case, it is concerned that linearity will be evident because the geometry of scintillator is irregular and optically unstable[13].

2) Plastic scintillator application

The plastic scintillator is a promising solid-state material to detect the beta ray. The background counting rate of the scintillation-based detector is relatively stable to the temperature and humidity. The plastic scintillator is physio-chemically stable, and its optical characteristic is not vulnerable to the environmental condition. Additionally, it is advantageous for beta ray measurements because of its low atomic number which can suppress backscattering and Bremsstrahlung effects and low mass density which can decrease the background counting rate from external gamma ray or cosmic ray [14].

The properties of plastic scintillators and other scintillators were compared. Table 1-1. presents the specifications of typical commercial scintillators (Saint-Gobain Crystals). NaI(Tl) and CsI(Tl), which are the most popular scintillators, were rejected because of their hygroscopic property. They are not suitable to detect extremely low-energy beta ray if protecting coat is required. Lutetium-yttrium oxyorthosilicate (LYSO(Ce)) and bismuth germanate (BGO) were rejected due to their high density. CaF_2(Eu) is the most competitive scintillator comparing to the plastic scintillator to detect the beta ray [15, 16]. It has relatively low density and no hygroscopic property. However, density is still higher than that of the plastic scintillator, and decay time was relatively high. Because a coincidence technique is required to detect the low-energy beta ray of tritium, decay time of 1,000 ns is too long to apply for coincidence. Time information of the generated pulse signal is important for the coincidence technique; thus the shorter length of the signal is more advantageous.

The BC-400 shown in table 1-1 is a typical model for general purpose. Various models can be selected according to the purpose, and the emission wavelength and time constant mainly vary depending on the model. For example, the BC-428 is a green emitter that its most probable wavelength is 480 nm, which are more responsive to the silicon photomultipliers or photodiode. Depending on the type of PMT, or specially requiring fast coincidence, it is necessary to carefully select the model of the plastic scintillator.

Table 1-1. Specifications of typical commercial scintillators (Saint-Gobain Crystals)

	NaI(Tl)	CsI(Tl)	LYSO(Ce)	BGO	CaF_2(Eu)	BC-400 (Plastic)
Emission wavelength (nm)	415	550	420	480	435	423
Decay time (ns)	250	1,000	36	300	940	2.4
Light output (photons/MeV)	38,000	54,000	33,000	8,000	19,000	10,000
Density (g/cm^3)	3.67	4.51	7.1	7.13	3.18	1.03
Hygroscopic	Yes	Slightly	No	No	No	No
Refractive index	1.85	1.79	1.81	2.15	1.47	1.58

A few studies about the on-line continuous monitoring of tritium in water using solid scintillator have been carried out. Jang et al. reports the remote and direct tritium measurement method using inorganic scintillator powder consolidated using epoxy and optical fiber bundle [17]. It has limitation of low detection efficiency thus it is applicable for GBq of tritium in water. Detection efficiency of direct measurement of tritium beta ray in water would be extremely low because of self-absorption effect [16].

Plastic scintillator plate was used to detect the continuous tritium-in-water detector with but the detection limit was low which can be applicable for GBq/L order of tritiated water like effluent in fusion reactor [18, 19]. Scintillator beads or fibers were adopted to increase effective area of the scintillator and obtain lower detection limit order 40 kBq/L in 1 h [13, 20]. However, theoretical detection efficiency based on the computational calculation was high, but it had problem in practical application due to optical transportation. In these reasons, an alternative way to detect the tritium is considered. Another study for increasing effective area of scintillator was reported by Uda et al [21]. It fabricated swirling flow-path made of plastic scintillator to increase the area contact with tritiated water and plastic scintillator. It showed detection efficiency of 0.32%, and detection limit of 1,430 Bq/cm^3. It was significant as an attempt to increase the detection efficiency by increasing the length of the flow path made of a plastic scintillator.

3) Gas-state tritium monitors

Gas-state tritium monitors has been commercialized. The representative types of detector are ionization chamber and proportional counter. The ionization chamber has been used to tritium in air[22]. Ionization chamber-based tritium monitors are installed in nuclear facilities to protect workers from tritium leakage accidents. The detection limit of the ionization chamber to the tritium is approximately few tens of kBq/m^3 for commercial models. However, because the operating principle of the ionization chamber is collecting extremely small amounts of current (on the order of fA), the technique is vulnerable to humidity and temperature which affect current delivery in the chamber [23, 24]. For this reason, its recording value fluctuates. Another method of tritium monitoring is using the proportional counter [25, 26]. Despite the low background counting rate and the low MDA of the proportional counter, it is difficult to use it for continuous tritium monitoring because the use of counting gas has certain problems; a large amount of counting gas, such as P-10 gas, should be mixed with the air sample to operate the proportional counter, and this lowers the stability of the recording results. Additionally, the use of consumables is not suitable for continuous monitoring.

A few studies reported detection of gas-state tritium using plastic scintillator. A disadvantage of the plastic scintillator for measurement of a beta ray emitted from the radioactive gas is its low detection efficiency. The beta ray interacts with the gas in the whole chamber of the gas-filled type detector; thus, the whole volume of the chamber is valid for detection. Because beta ray interacts only when entering the scintillator, detection of low-energetic beta ray is valid only in short range around the scintillator. Furuta and Ito reports the tritium measurement in expired air (vapor) using plastic scintillator pellets [27]. The plastic scintillator pellet was adopted to increase the effective area for interaction and adhesion with HTO and plastic scintillator. The detection efficiency was less than 5% and detection limit was 240 Bq/L (in vapor) with measurement time of 10 min.

4) Gasification of tritiated water and detection

Gasification of the water can increase detection efficiency thought the volume of the sample is increased and concentration of tritium dropped. Khenari reported the tritium detection system by boiling the water sample using ionization chamber which has detection limit of 740,000 Bq/L in 10 s [28]. The condition of operation of the system would be complicated because the temperature and humidity should affect the detection properties. Another gasification method other than evaporation is gasification through electrolysis. Soreefan reported a PEM electrolysis-based tritium monitor using a gas-flow proportional counter [29, 30] where the detector had detection limit of 740 Bq/L in 1.5 h of electrolysis followed by 4 h counting. The gas-flow proportional counter has been shown to consume a counting gas comprising methane and argon. Furthermore, the tritiated gas should be carefully mixed with the counting gas using syringe pump. Therefore, in consideration of the constant need for consumables and uncertainty due to mixing gas, it is not suitable for continuous monitoring and analysis of large tritiated samples. However, the approach to the gasification of the water sample using electrolysis was significance.

The concentration of tritiated hydrogen gas generated through electrolysis can be quantified by fractionation factor. Characterization of the fractionation factor is important to convert the tritium concentration in liquid to gas. Roy reports that the fractionation factor was varied by temperature of tritiated water [31]. In the study, energy of the liberation of the isotopes in hydrogen-tritium system by the difference in the free activation energy for transfer of proton to the cathode and triton to cathode. The difference in activation energy was -2260 cal/mole for hydrogen-tritium system. The system is exothermic, and it implies that the fractionation factor decreases as the temperature increases though the study was carried out in Ni-Fe.

1.3 Purpose of the Study

The purpose of the study was development of on-line continuous monitoring technology of tritium in water with continuous inflow of the sample. The existing method of detecting tritium in water was to contact the scintillator directly with the water sample. Because this method has very low detection efficiency, it is difficult to obtain a low MDA. There was a case in which gasification using electrolysis and a proportional counter are applied, but it was a method that was applicable at the laboratory level and hard to use it outside. Therefore, in this study, a plastic scintillator-based detector with enhanced detection efficiency was fabricated to detect gasified tritium which was generated through electrolysis. PEM cell-based was used to electrolyze the tritiated water and gasify it, and plastic scintillator-based detector was mounted in series. High detection efficiency and stability were required to meet this purpose. PEM cells generate hydrogen gas through the electrolysis of water. Because there is no need to add an additional electrolyte, it is environmentally friendly and reusable. A plastic scintillator, which does not generate many bremsstrahlung radiation and has low probability of interacting with external gamma rays because of low atomic number (< 4), volumic mass density (~1 g/cm^3), and resistance to moisture, was selected as the tritium detecting material. Due to these characteristics, the combination of electrolysis and plastic scintillator was thought to be suitable for continuous monitoring of tritium in water. The proposed system can continuously monitor tritium in the water without consuming disposable products or polluting the environment with hazardous materials. Also, drained water after analysis is not chemically contaminated. Additionally, purification prior to the electrolysis and generation of hydrogen gas can fundamentally reject the disturbance due to other radionuclides.

In chapter 2, fundamental test of tritium detection using plastic scintillator was carried out. A sealed tritium surficial source and a planar plastic scintillator were used. Energy calibration was carried out using single PMT, amplifier and multi-channel analyzer (MCA). Coincidence spectrum was obtained using coincidence circuit system and range of interest was investigated to reject the worthless noise signal counts. By giving the offset between the scintillator and the source, the change pattern of the counting rate was analyzed.

In chapter 3, the electrolysis characteristics of tritiated water using PEM cell was evaluated. This part includes the experiments to obtain correlation between the concentration of tritiated water and the concentration of tritium gas generated after electrolysis. Electrolysis system was developed, and a commercial gaseous tritium detector was utilized. Additionally, preliminary home-made tritium detector was fabricated and conceptual verification for continuous tritium detecting method was conducted using the electrolysis system and the detector.

In chapter 4, multi-channel plastic-based tritium detector was designed. The plastic scintillator detector, fabricated in the previous part, includes only two scintillators and their diameter was 50 mm which was fit with 2-inch-window PMT. Therefore, volume of the chamber relatively small and the detection efficiency was low, too. Design of multi-channel type, which means narrow flow channels were parallelly placed, can effectively increase the detection efficiency. The multi-channel detector was designed by giving variety to design parameters such as number of the channel and thickness of the plastic scintillator and their performances were tested using a computational simulation code. A prototype multi-channel detector was manufactured to have the maximum performance at the level that can be actually processed, and its detection efficiency was estimated.

In the chapter 5, a prototype system was developed and tested for the capability of real-time on-line continuous tritiated water monitoring. The system was designed by combining the electrolysis characteristics obtained in the part I and the detection chamber newly developed in part II. The design of the system was carried out based on the conditions to achieve the theoretical maximum performance, and the detection efficiency and MDA of the final system after combining the electrolysis with PEM cell and the detection part were evaluated. Then, it includes discussions on the operation method of the system applicable to practical fields such as tritium monitoring in drainage facilities during nuclear power plant operation, environmental survey for decommissioning of nuclear power plant, etc.

Chapter II. Fundamental Tests for Tritium Detection

2.1 Plastic Scintillator for Tritium Detection

Beta ray interacts with a scintillator and photons are produced. The number generated photon is proportional to the absorbed energy into the scintillator. The generated photon is converted by using the light detecting apparatus and the pulse signals are counted using pulse height analysis. Fig 2-1 present principle of detection of low-energy beta ray using plastic scintillator.

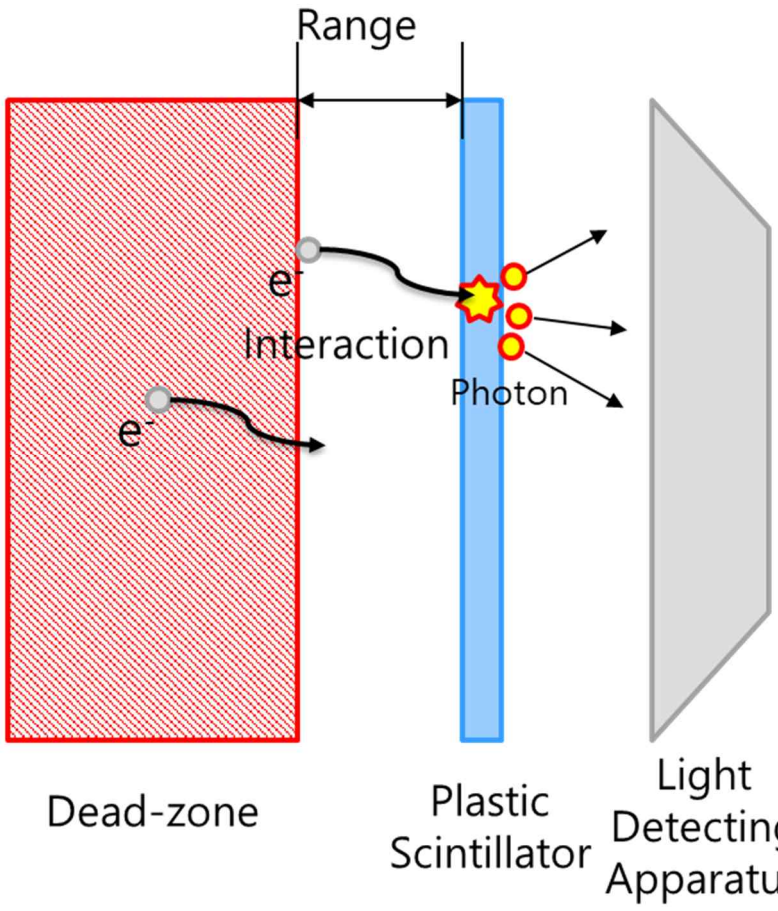

Fig. 2-1. Principle of detecting low-energy beta ray using plastic scintillator

In case of detecting low-energy beta ray, such as tritium, range (the distance of flight) is extremely short. When a radioactive isotope decays at the shorter distance with plastic scintillator than its beta ray's range, the beta ray can interact with the plastic scintillator and produce photon. Otherwise, when it decays distant from the scintillator, the beta ray can't interact with plastic scintillator and it cause decrease of efficiency. If medium is water, the range of tritium beta ray is less than few tens of μm, the detection efficiency will order of 10^{-5}. The water medium should be thin to increase the detection efficiency, but the volume of the sample will be extremely small as well as hydrodynamical difficulty. If medium is hydrogen gas, the range of tritium beta ray would be few mm. In other words, aerodynamical design to allow gas to flow well and to have a detection efficiency order of 10^{-1} is expected to be possible. Because of these aspects, the detection of beta-rays of tritium in gas was desired.

Additionally, because the energy of tritium beta ray is extremely low, their pulse height is low. Discrimination of between the desired pulse and noise signal is important to maximize the detection efficiency and reducing the counting rate. A fundamental experimental setup was prepared for testing principle of tritium detection using plastic scintillator. Light detecting apparatus was composed using PMT, amplifier and time resolving system.

Basic computational simulations and experiments were performed to obtain the detector design elements. Frist of all, Proper thickness of scintillator was obtained by computational simulation using MCNP6. And single PMT was used to acquire energy spectrum using the plastic scintillator. Through the energy spectrum, the required gain in the combination of the plastic scintillator and PMT was approximately estimated, and the detectability of tritium was experimentally verified. The coincidence circuit was composed and tested. Before using the gaseous tritium source, the efficiency that can be obtained from the planar plastic scintillator was evaluated using a sealed surficial tritium source which has relatively stable emission rate.

2.2 Computational Simulation of Tritium Detection

Before starting the experimental works, computation simulation was carried out to find 1) proper thickness of the scintillator and 2) approximate detection efficiency for comparison the experiment result. In general, a beta ray range model was defined with empirical expression as shown in Eq (2.1) and Eq. (2.2) [32].

$$R_\beta = 0.407 E^{1.38} \quad E_\beta \leq 0.8\ MeV \tag{2.1}$$

$$R_\beta = 0.542E - 0.133 \quad E_\beta \geq 0.8\ MeV \tag{2.2}$$

where R_β and E_β are range in g/cm^2 and the energy of the beta ray. This expression fits well at energies that do not deviate significantly from 0.8 MeV. However, tritium emits extremely low energy of beta ray with 5.7 keV in average and 18.6 keV in maximum. When this energy is applied to Eq (2.1) above, the average and maximum range is calculated as 0.0078 g/cm^2 and 0.0400 g/cm^2, respectively. By considering the density of the plastic scintillator presented in table 2-1, the thickness of the plastic scintillator for the tritium beta ray are 75.83 μm.in average and 387.9 μm in maximum, respectively. This value was expected to be overestimated because beta ray with lower energy loss its energy drastically[33]. Therefore, particle transportation simulation was carried out using Monte Carlo N-Particle 6 (MCNP6) to verify the effective range of the tritium beta ray in the plastic scintillator medium [34].

Fig. 2-1 presents the overall simulation geometry. The dimensions of each part (sealed source, active area of the source and plastic scintillator) were same with the experimental setup described in section 2.3 except for the thickness of the scintillator. The size of the plastic scintillator was 50 × 50 × 10 mm. The thickness was thick enough to record beta ray track. The plastic scintillator was composed of H/C ratio of 1:1.10 and its density was set by 1.05 g/cm^3. Because the material information of the sealed tritium source was not published, it was assumed aluminum with density of 2.7 g/cm^3. The source

distribution was carefully set to be uniform over a circle in the sealed source part using an option of special source probability function. The air gap between the scintillator and the source was set by 10 μm. The source information for the beta ray energy of tritium was obtained from radiological toolbox [35].

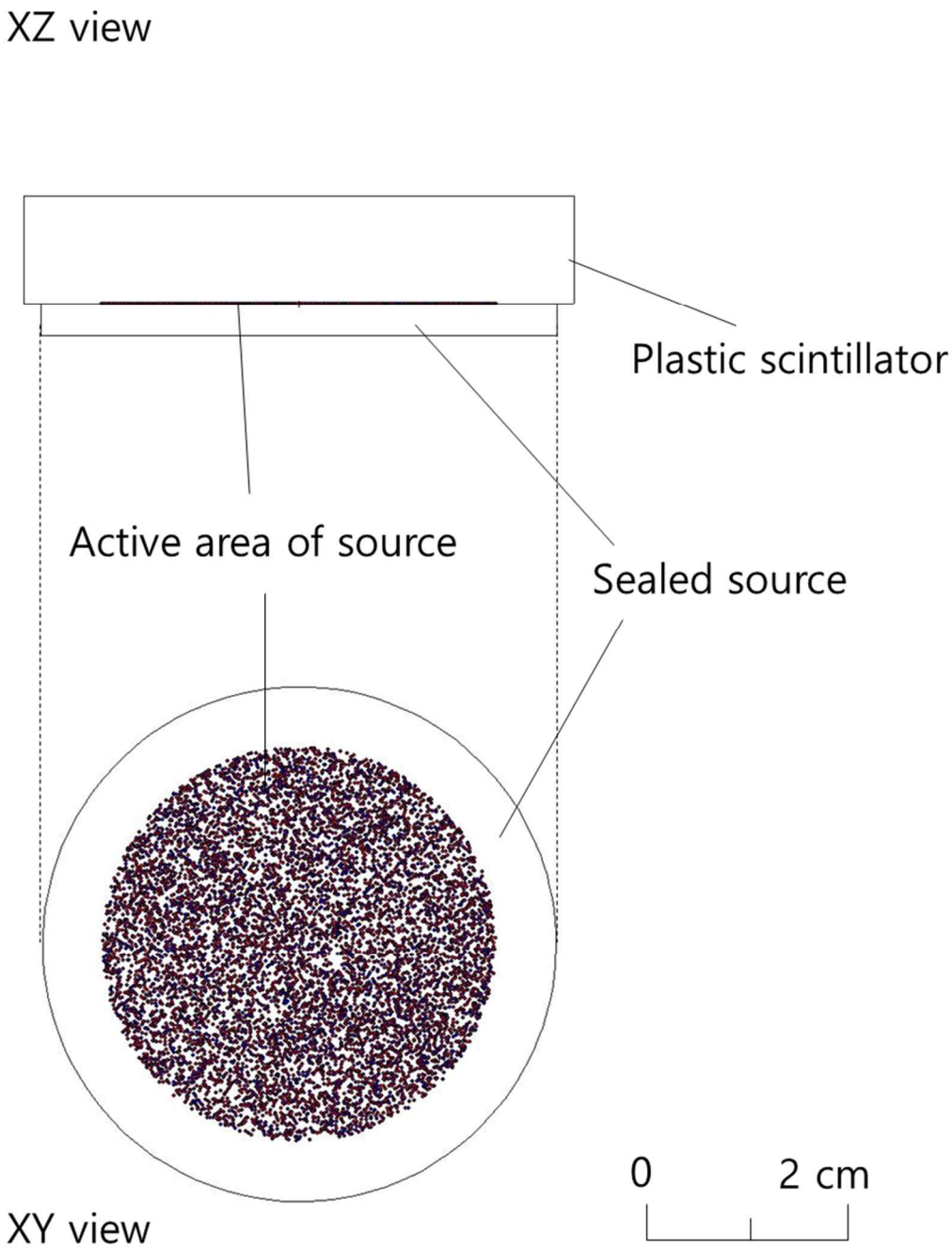

Fig. 2-2. The overall simulation geometry with XZ-plane view (upper) and XY-plane view (down)

2.3 Experimental Setup

Fig. 2-2 shows the detection chamber and light detecting apparatus to count the signals produced by the interaction between beta ray emitted from the tritium and the plastic scintillator. The light detecting apparatus was based on the coincidence measurement circuit. Coincidence circuit is utilized to selectively detect the light signals generated due to ionizing radiation and reject the background noise signals. The photons produced by the interaction between beta ray and the scintillator are incident to the two facing photomultiplier tubes. The photon is isotopically generated in a scintillator, it is expected to the both photomultiplier tubes detect the light signal at the same time. To record the time information, timing single channel analyzer (SCA) which can convert the input signal by sharp and distinct timing signal is required. And delay modules delay is utilized to make time difference of given time interval.

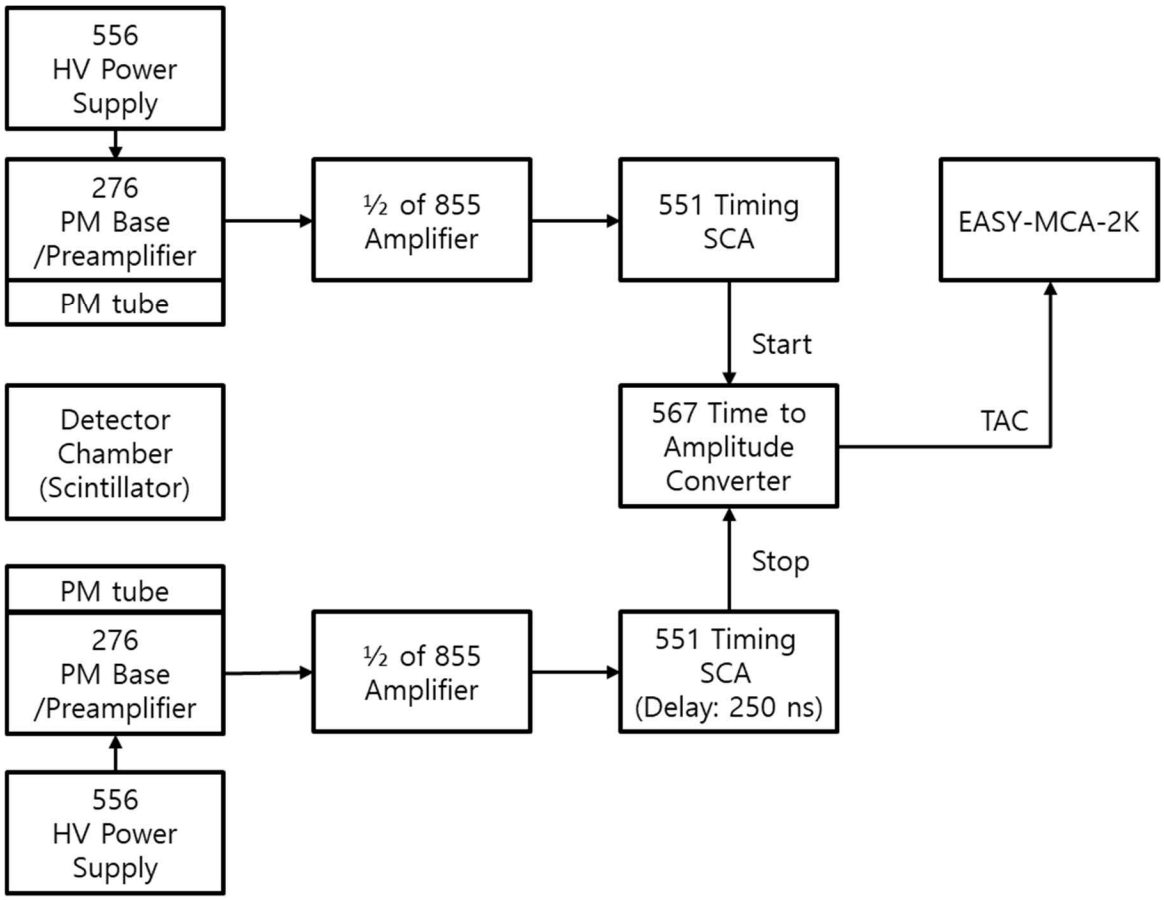

Fig. 2-3. A conceptual diagram of light detecting apparatus with coincidence circuit

The time difference between two signals is converted to a voltage signal by the time to amplitude converter (TAC). The output of the TAC is transported to the multi-channel analyzer (MCA), and the spectrum data are recorded by discriminating the voltage signal from 0 to 10 V into the whole number of channels. Using the spectrum data, the optimized window of the timing signal is selected. For example, full range of the output signal from TAC is set by 0 to 500 ns, if the MCA has 1024 channels, a single channel indicates about 0.488 ns. In this case, the signals with time difference of 250 ns will be recorded in the 1024^{th} channel.

Fig. 2-3. Shows the experimental setup of the fundamental tritium detectability test. The light detecting apparatus was composed of two PMTs (R878, Hamamtsu photonics) and signal processing units which is displayed in Fig. 2-1. The PMTs are mounted in a dark box and sealed to block the external light. The tritium source and plastic scintillator was parallelly placed.

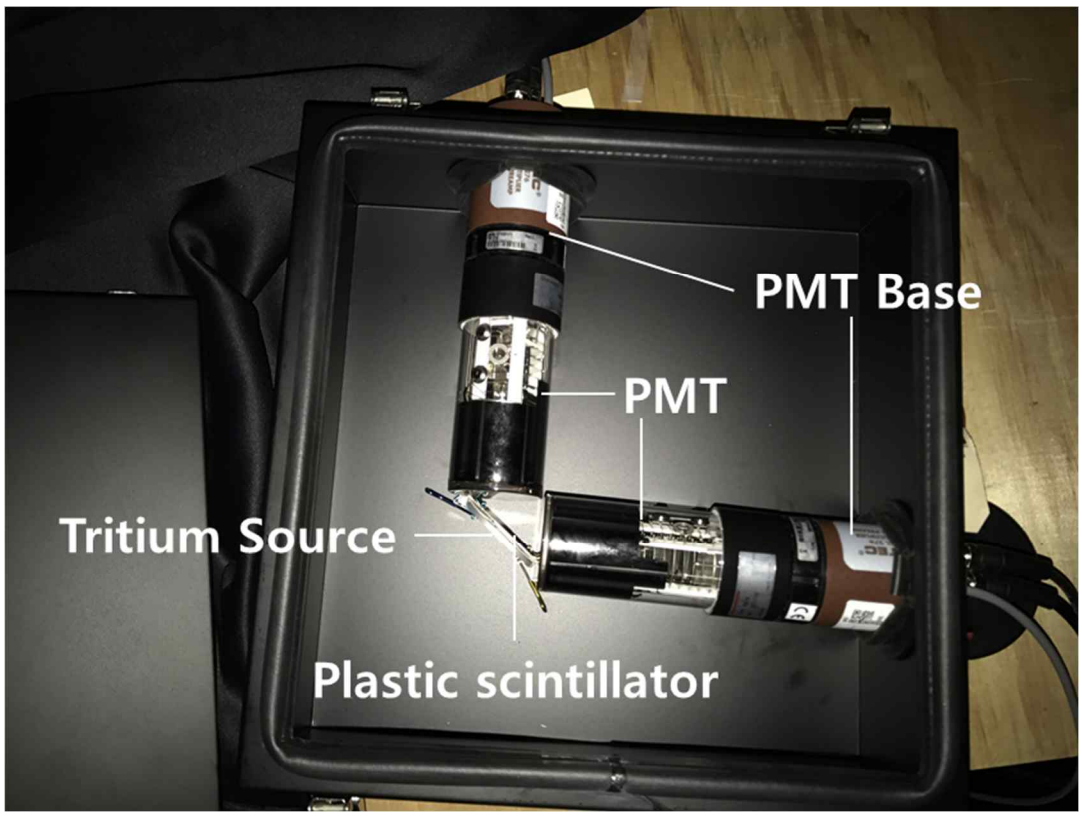

Fig. 2-4. Experimental setup of the fundamental tritium detectability test

The plastic scintillator was supplied by Epic-crystal and its specification is described in Table 2-1. The decay time of the plastics scintillator was short enough to make a coincidence system while the decay time of the PMT was much longer (80 ns). The wavelength of emission peak was 415 nm which was match to the general bialkali-type PMT such as R878. The dimension of the plastic scintillator was 50 mm × 50 mm × 1 mm. The width of 50 mm was selected by considering the window size of the PMT.

Table 2-1. Datasheet of the plastic scintillator (Epic-Crystal)

Parameters	Values
Density (g/cm^3)	1.05
Decay time (ns)	2.40
Light output (%relatively of Anthracene)	50-60
Soften temperature (K)	348
Wavelength of emission peak (nm)	415
H/C ratio	1.10
Refractive index	1.58
Hygroscopic	No
Cleavage	No

The sealed tritium source supplied by Eckert&Ziegler and its specification is described in Table 2-2. The corrected surface emission rate was calculated considering radioactive decay. The diameter of active window was 36 mm which was smaller than the diameter of PMT window (50 mm) as well as the dimension of the plastic scintillator.

The first experiment was energy calibration using single PMT. A preamplifier and an amplifier were connected to an PMT and the output signal was directly connected to the MCA, not using the timing SC and TAC. In this composition, the energy spectrum can be acquired.

Table 2-2. Datasheet of the tritium surficial source

Parameters	Values
Radioactivity	10.0 kBq
Surface emission rate (in certificate)	192 s^{-1}
Corrected surface emission rate	189 s^{-1}
Overall dimension	Φ 47 × 3 mm
Active dimension (window)	Φ 36 mm
Uncertainty of beta surface emission rate	6%

Therefore, x-axis of the spectrum means the absorbed energy by interaction of beta ray and scintillator. The tritium source and ^{14}C source (370,000 Bq) was used for energy calibration. ^{14}C is a pure-beta emitter that its maximum energy is 156 keV. Using the beta ray spectrum, energy calibration of the plastic scintillator was carried out. The gain was set by 80, by adjusting the coarse gain as 20 and fine gain as 4. The measurement was carried out for 300 s.

The second experiment was coincidence circuit test. Using the coincidence circuit, timing spectrum can be obtained and its range of interest (ROI) was set. The counting rate in ROI was considered to estimate the detection efficiency of the detector. To acquire the ROI, full width at half maximum (FWHM) of the peak for the ROI was used. Primarily, the center of the plastic scintillator and the tritium source was aligned and adhere them together. After ROI was obtained, offset test was carried out. By the offset test, it was expected to estimate the approximate range of the beta ray of tritium. The axis direction offsets between the plastic scintillator and the source were 0, 1 and 5 mm, respectively. The side direction offset between the plastic scintillator and the source were 0, 10 and 20 mm, respectively. The gain was set by 240, by adjusting the coarse gain as 40 and fine gain as 6. The measurement was carried out for 300 s.

2.4. Results and Discussion

Fig. 2-4 shows the particle track simulation result of tritium beta ray and plastic scintillator. The maximum track length was about 10 μm and the length of penetration was less than 5 μm. Comparing with the values that derived from the empirical expression, they were much shorter. It was thought that the specific energy loss in lower energy was exceedingly high thus the range was very short. Therefore, the required thickness of the plastic scintillator to avoid escaping of beta ray was very thin; few tens of micrometers were enough.

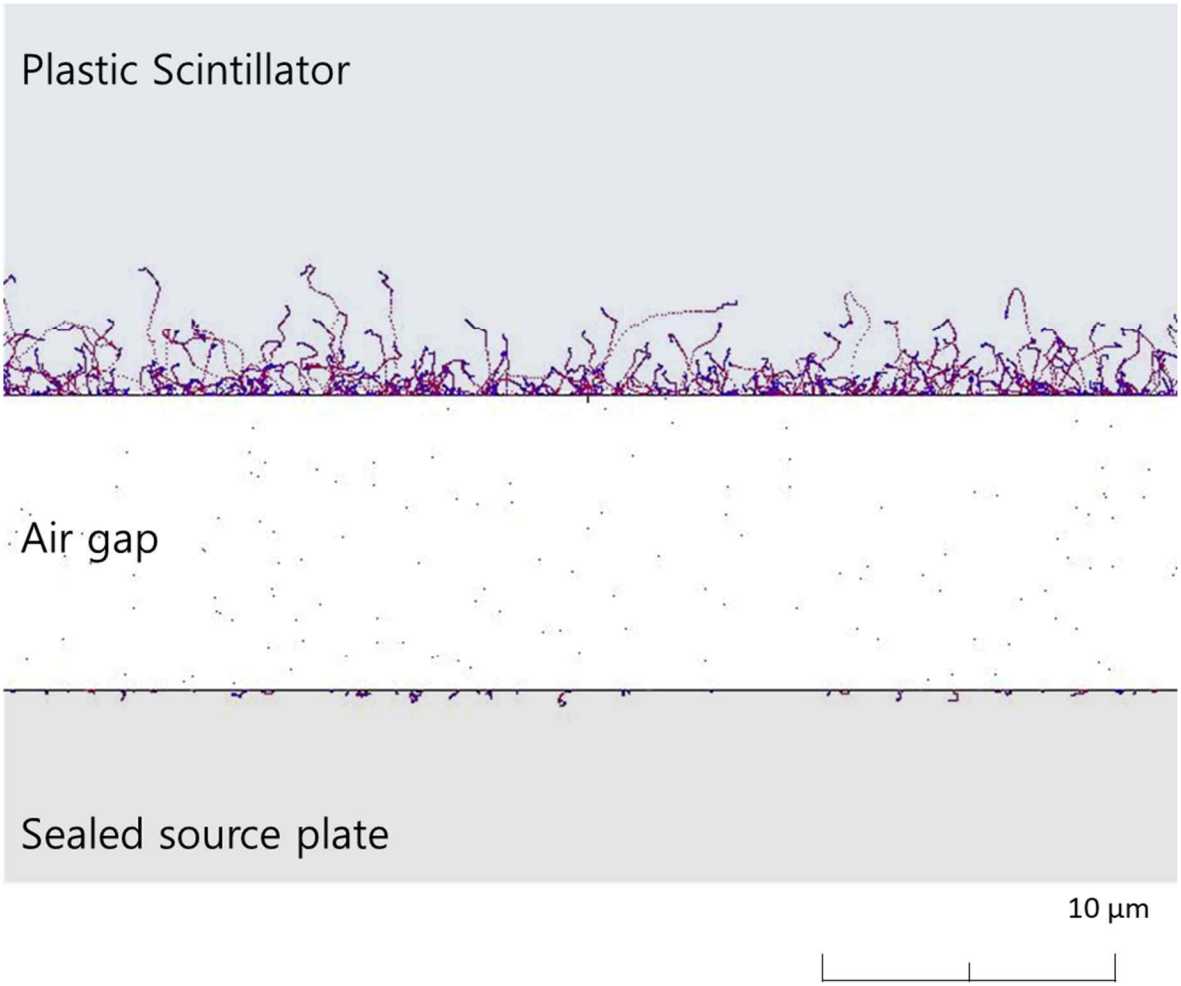

Fig. 2-5. Particle track simulation result of tritium beta ray and plastic scintillator

Fig.2-5 presents the acquired beta ray spectra using ^{14}C and ^{3}H sources. The number of counts in channels were normalized because the activities of the sources were different. The from 1 to 748

channel contains 99.99% of total counts. Therefore, the 748-th channel was considered as 156 keV, and energy-channel ratio was evaluated by 0.209 keV/Ch. Using this, the channel number which indicated 18.6 keV was 89 Ch. The detection efficiency for the tritium was estimated by 34.49±2.08%. This detection efficiency was obtained in the condition that the plastic scintillator and the sealed tritium source were tightly closed. It is not a meaningful number and can be interpreted as the maximum detection efficiency that can be obtained in an ideal environment. The background counting rate was estimated by 22.36 cps.

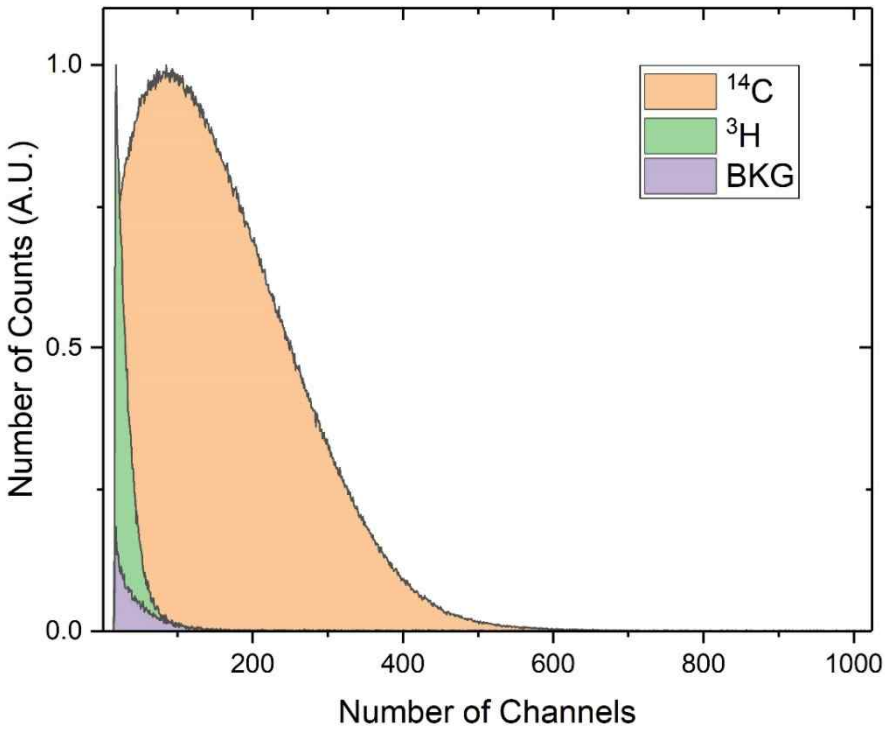

Fig. 2-6. Beta ray spectra acquired through experiment using sealed ^{14}C and ^{3}H sources. The number of counts were normalized.

Fig. 2-6 presents the tritium spectra acquired from the simulation (orange) and the experiment (green). In the spectrum obtained from the simulation, energy bin for recording the particle (tally) was based on the experiment. The energy range was set by 0 to 0.156 MeV and they were segmented by 784. The

detection efficiency was 58.9%, which was much higher than that of obtained from the experiment. Compared to the simulation results, in the experiment, the lower energy part of the spectrum was dominant. Because the peak was formed lower than the average energy of tritium beta ray, 5.7 keV, this is considered to be due to the self-absorption of the sealed source. Many signal counts were cut off in the low energy part. Therefore, the need for coincidence circuit to reduce the noise signal with more amplification was highlighted.

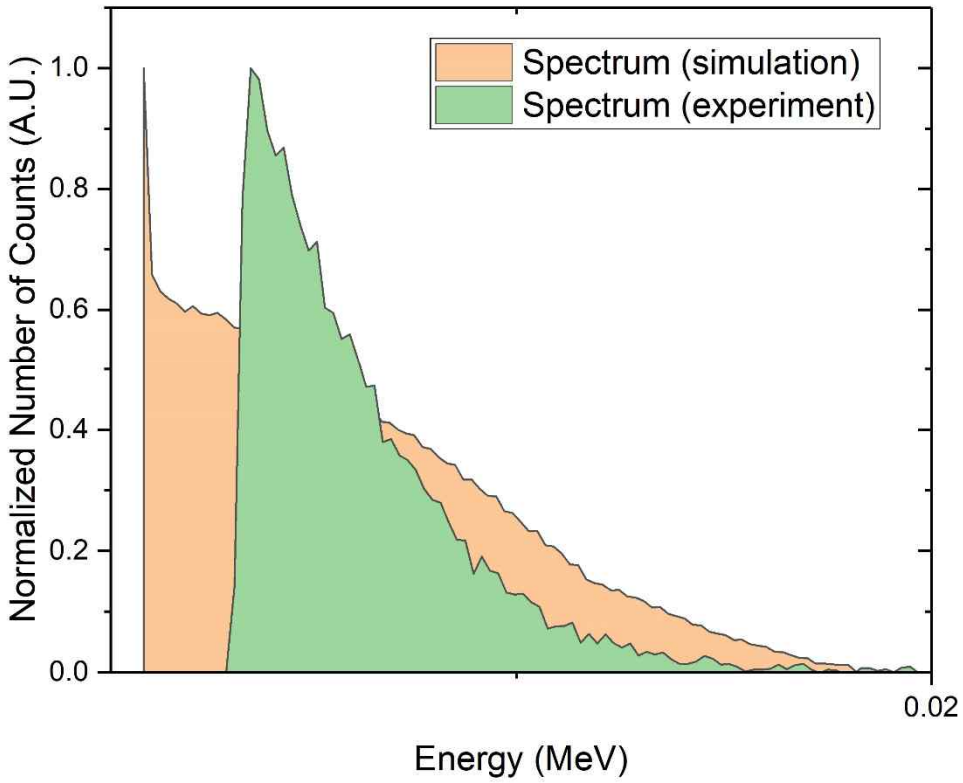

Fig. 2-7. The tritium spectra acquired from the simulation (orange) and the experiment (green).

Fig. 2-7 (a) presents the coincidence spectra that obtained without tritium sealed source and Fig. 2-4 (b) that with a plastic scintillator with tritium sealed source. The x-axis of the spectrum indicates time difference between start and stop signals for the input of the TAC. Because the full window range was set by 500 ns and time difference was set by 250 ns. FWHM of the peak was 140 Ch, which corresponds

to the 68.36 ns. By considering the decay constant of the PMT was 80 ns, the width of the peak makes sense. The ROI was set by doubling this, from 268 to 651 Ch to contain 2σ range (approx. 95%) of the peak.

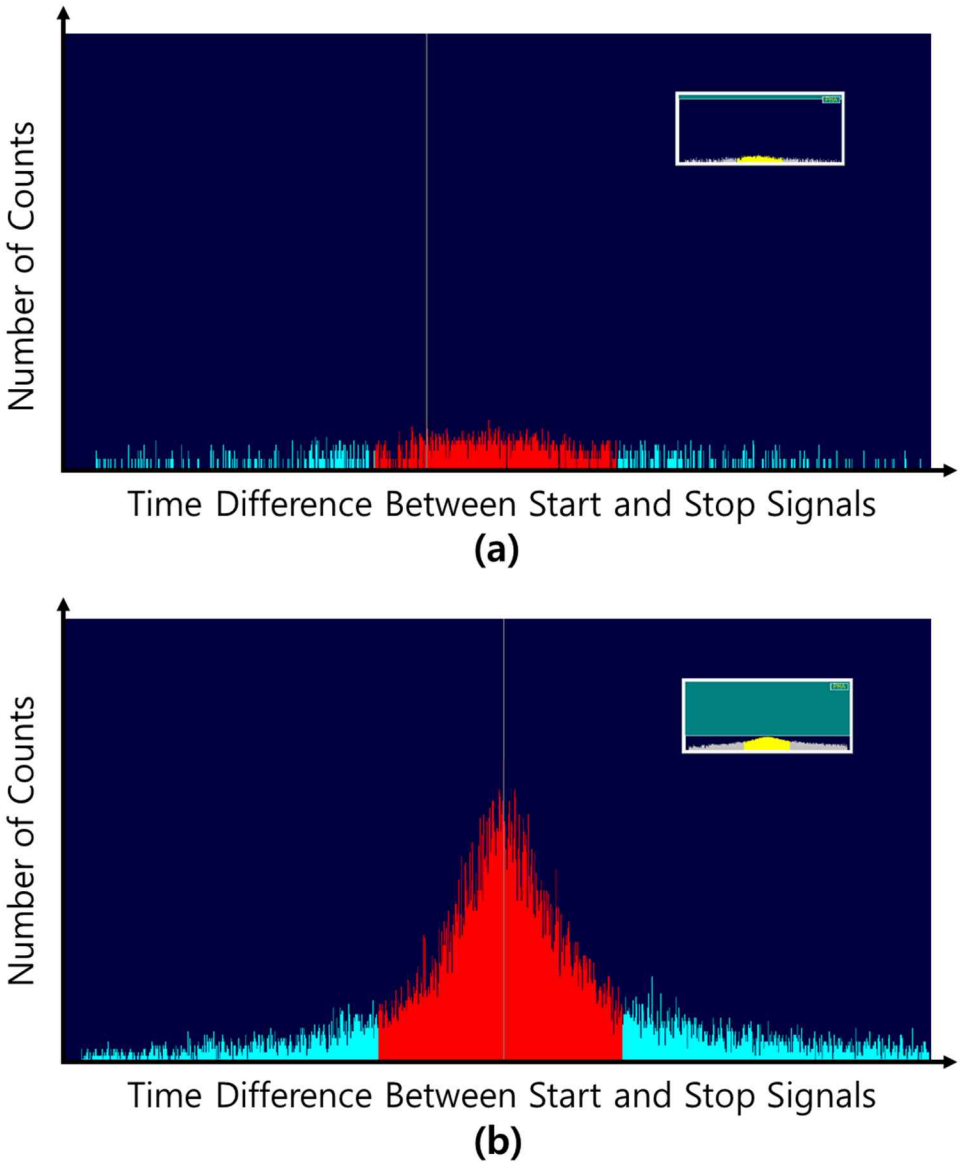

Fig. 2-8. Coincidence spectra in case of no scintillator (a) and scintillator with tritium source (b)

Table 2-3 presents the counting rates and detection efficiency with different source positions. The background counting rate was 12.66 cps. The background counting rate was decreased thought the gain was increased because of coincidence circuit. Otherwise, the detection efficiency was decreased

comparing with the single PMT system. There are two reasons for this. First, the optical efficiency was lowered because the PMT and the plastic scintillator are not attached in the experimental arrangement. The second reason was that some of the signals were eliminated in the coincidence circuit. Some signals should be laid out of ROI. This experiment is significant in that it is an experiment to check whether the coincidence circuit works well when using a plastic scintillator.

Table 2-3. Counting rates and detection efficiency with different source positions

Source position		Counting rates (cps)	Net counting rates (cps)	Detection efficiency (%)
Center		64.95	52.29	27.67
Offset – side direction	10 mm	57.03	44.37	23.48
	20 mm	47.51	34.85	18.44
Offset – axis direction	1 mm	23.02	10.36	5.48
	5 mm	19.49	6.83	3.61
Background		12.66	-	-

2.5 Summary

A fundamental study for tritium beta ray measurement using plastic scintillator was carried out. The particle transportation simulation was carried out to obtain the required thickness of the plastic scintillator and the theoretical maximum detection efficiency. The range of the tritium beta ray was much shorter than the calculated by the empirical expression, as expected. It was confirmed that very thin plastic scintillator can be used. The detection efficiencies between the simulated and experiment results were quite different as well as the shape of the energy spectrum. The primary reason was thought to be limitation of the sealed source because the source itself absorbs the energy of the beta ray. The energy calibration was carried out using single PMT system. The maximum energies of the spectra were linear for ^{3}H and ^{14}C. Coincidence circuit was prepared and tested with the sealed tritium source. The time difference spectrum obtained by the coincidence circuit appeared similar to the expected result. The signal counts were concentrated in the center, which corresponds to the given time difference. The ROI was set using FWHM. Through this experiment and simulation, the required thickness of the scintillator and expected efficiency of the plastic scintillator for tritium measurement were obtained, which was later used in the design of a detector for measuring gaseous tritium.

Chapter III. Electrolysis Characteristics of Tritiated Water and Preliminary On-line Continuous Tritiated Water Monitoring System

3.1 Electrolysis Characteristics of Tritiated Water

Electrolysis has been used in radiochemistry to enrich the tritium in water in order to measure extremely low levels of tritium [36]. Therefore, the hydrogen gas produced via conventional electrolysis does not contain much tritium, and most of the tritium remains in the water. In contrast, the hydrogen gas produced via PEM cell-based electrolysis contains more tritium than that produced via conventional electrolysis techniques. Depending on the method of electrolysis, tritium or hydrogen atoms are separated from the form of water to form a gas. The fractionation factor determines this characteristic which is defined as a ratio of separated proton atoms to hydrogen atoms during electrolysis. Soreefan et al. reported that the produced gas using the PEM cell-based electrolysis contained more tritium than conventional electrolysis such as Ni/Fe-based conventional electrolysis [29]. PEM-based electrolysis shows the fractionation factor ~5 while Ni/Fe-based conventional electrolysis shows the fractionation factor of ~25 [37, 38]. This implies that the PEM-based electrolysis can evolve more tritium then conventional electrolysis.

In this chapter, characterization of PEM electrolysis cells for online continuous monitor for large tritiated water samples was conducted. In the Soreefan's work, volume change before and after electrolysis is a key factor for estimation of the fractionation factor. However, measurement of the volume is not precise thus the relative error was large. An alternative method to evaluate the fractionation factor with less relative error was suggested. Fractionation factor was estimated by evaluating the linearity between the tritium concentration of the produced gas and the tritiated water sample. In addition, one of the factors that can affect the fractionation factor is temperature. Therefore, the fractionation factor was estimated according to the temperature of the tritiated water sample. This

will contribute to lowering the MDA of the developing monitoring system through optimization of the fractionation factor.

3.2 Definition of the Fractionation Factor

Conventional electrolysis using aqueous electrolyte enriches the tritium in water, and thus, only the hydrogen atom (proton), not the tritium atom (triton), is converted into gas. However, electrolysis using a polymer electrolyte membrane (PEM) can gasify the tritons, thus providing more tritium. This characteristic is defined as the fractionation factor (β), which is expressed as the ratio of the number of protons to the number of tritons converted to gas during electrolysis. The lower fractionation factor—close to unity—implies more tritium is present in the gas produced by electrolysis.

The original purpose to estimate the fractionation factor is to evaluate the exact degree of enrichment. In the aspect of enrichment, the fractionation is defined as shown in Eq. (3.1)

$$E = \frac{T}{T_0} = \left(\frac{V_0}{V}\right)^{1-\frac{1}{\beta}} \tag{3.1}$$

where E, T_0, T, V_0, V are enrichment factor, initial and final concentration of the tritium in water, and initial and final volume of the tritiated water sample, respectively. However, it was thought that the relative error was large because the volume was difficult to measure accurately and could change due to heat generated during the electrolysis process.

Although the PEM cell has these advantages, concentration changes due to gasification and ratio of proton-triton selectivity (fractionation factor) should be considered. The tritium concentration in an electrolyzed gaseous sample (T_{gas}) can be derived as shown in Eq. (3.2).

$$T_{gas}\left[\frac{Bq}{m^3}\right] = T_{liquid}\left[\frac{Bq}{L}\right] \times \left(\frac{V_0}{V}\right)^{1-\frac{1}{\beta}} \times \frac{1}{\kappa}\left[\frac{L}{m^3}\right] \times 1000 \times \frac{1}{\beta} \tag{3.2}$$

where T_{liquid}, κ, β, and are the tritium concentration in the liquid sample to be electrolyzed, the hydrogen volume correction factor during the electrolysis and the fractionation factor. If the volumetric change of the tritiated water sample is ignorable, the term $\left(\frac{V_0}{V}\right)^{1-\frac{1}{\beta}}$ in the Eq. (3.2) goes to the unity. Then, the relationship between the tritium concentrations of liquid and gaseous hydrogen was expected to be linear, meaning that the slope would be the $\frac{1000}{\kappa\times\beta}$. Because the hydrogen volume correction factor was a constant at the same temperature and pressure; 7.36×10^{-4} in 25℃ at 1 atm. If the slope of the relationship can be evaluated by measuring the gases tritium concentration generated by electrolysis versus the liquid tritium concentration, it can lead to the estimation of the fractionation factor.

The fractionation factor depends on various parameters: electrode material, current density, and temperature [39-41]. In the aspect of electrode material, it has been reported that the PEM-based electrolysis, using solid membrane with electrode of Pt-Ir, showed lower fractionation factor than the conventional electrolysis compared with the conventional Ni-Fe electrode based aqueous electrolysis. The electrode material and current were not changed or controlled, because they are highly related to the hydrogen production rate. Sufficient hydrogen production rate was required for the continuous monitoring of the tritiated water. Therefore, the temperature was controlled to decease the fractionation factor.

3.3 Experimental Setup

Fig. 3-1 shows a conceptual diagram of the preliminary tritium monitoring system with electrolysis cell, and Fig. 3-2 shows a picture of the electrolysis system which consisted of an electrolysis cell, a power supply, a water pump, a sample container, and a hydrogen buffer. A 10-stack PEM cell with Pt-Ir catalytic electrode (WESPE Co., Ltd., Korea) was used. Power supply (TDP-3020B, Toyotech, Viet Nam) was used to apply a constant current of 7 A. The hydrogen gas production rate for this condition was 0.49 L/min, and its corresponding disintegration rate of water was 23.8 mL/h. The water pump transported the water from the sample container to the electrolysis cell and mixed the water sample so that the temperature became homogeneous. The sample container and hydrogen buffer were cylindrical in shape with volumes of 10.5 L and 1.3 L, respectively. A mass flowmeter (M2030V, Line-Tech, Korea) was provided to measure the amount of hydrogen gas generated. A commercial water heater was used to heat the tritiated water sample, and a thermometer was placed in the sample container to monitor the temperature. The temperature was controlled from 30 to 90 ℃. The room temperature and relative humidity were well-controlled to 24 ℃ and 61%, respectively, with an air conditioner. The initial temperature of the tritiated water sample was approximately 28 ℃ without external heating due to the amount of heat generated in the electrolysis cell. In this system, the produced hydrogen gas is transported through a stainless-steel tube. An ionization chamber-based tritium monitor was connected to the detection chamber exit to monitor the tritium concentration of the exhausting hydrogen gas to confirm the operation of the electrolysis system.

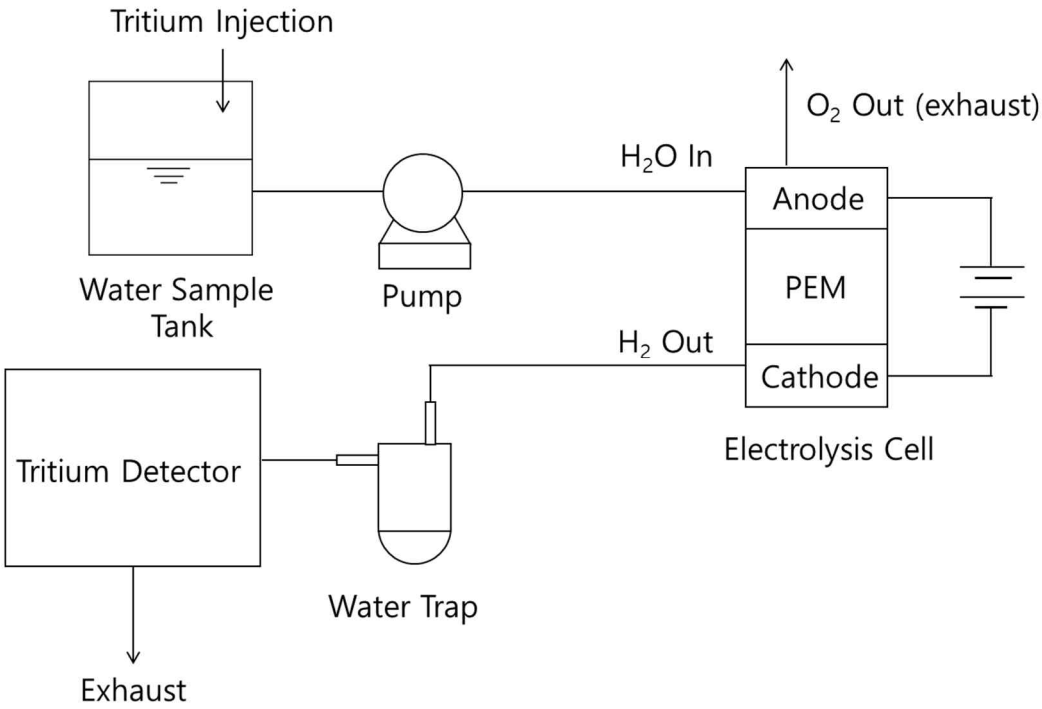

Fig. 3-1. Conceptual diagram of the preliminary tritium monitoring system and experimental setup

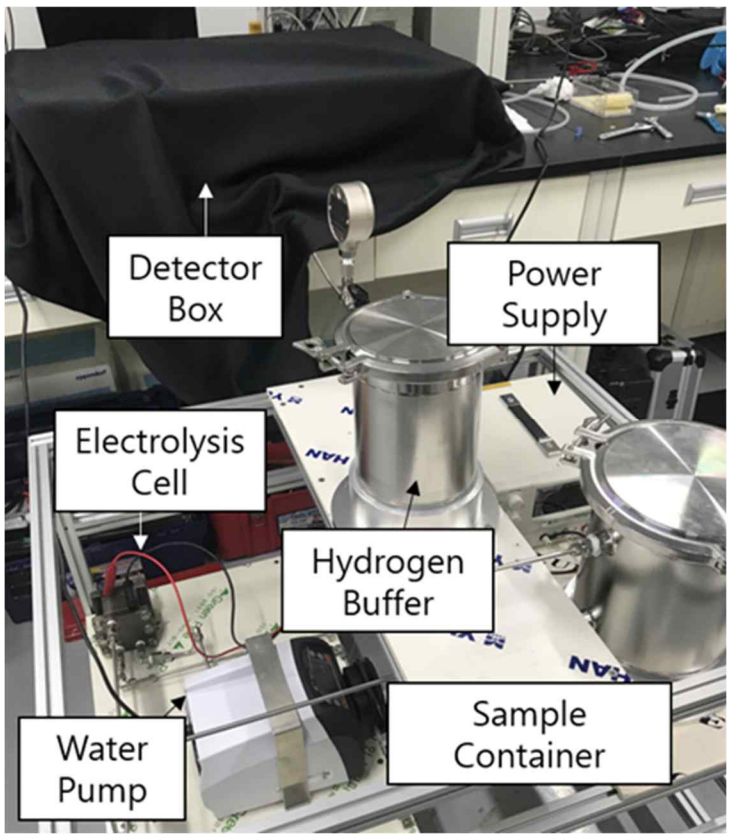

Fig. 3-2. Picture of the electrolysis system for tritiated water

A simple type of tritium detector consisting of two scintillators facing each other was connected to an electrolysis system to test the performance of the preliminary tritiated water monitoring system. Fig. 3-3 shows the preliminary tritium gas detector using plastic scintillator. Two plastic scintillators (Plastic scintillator, Epic Crystal) with diameter of 50 mm were attached with acrylic structure using optical cement (BC-600, Saint-Gobain Crystals). The acrylic structure has two flow path connections, and the space surrounding the plastic scintillators and acrylic structure becomes the volume of the detection part. The plastic scintillators are optically connected with photomultiplier tubes with window diameter of 50.4 mm (R878, Hamamatsu photonics).

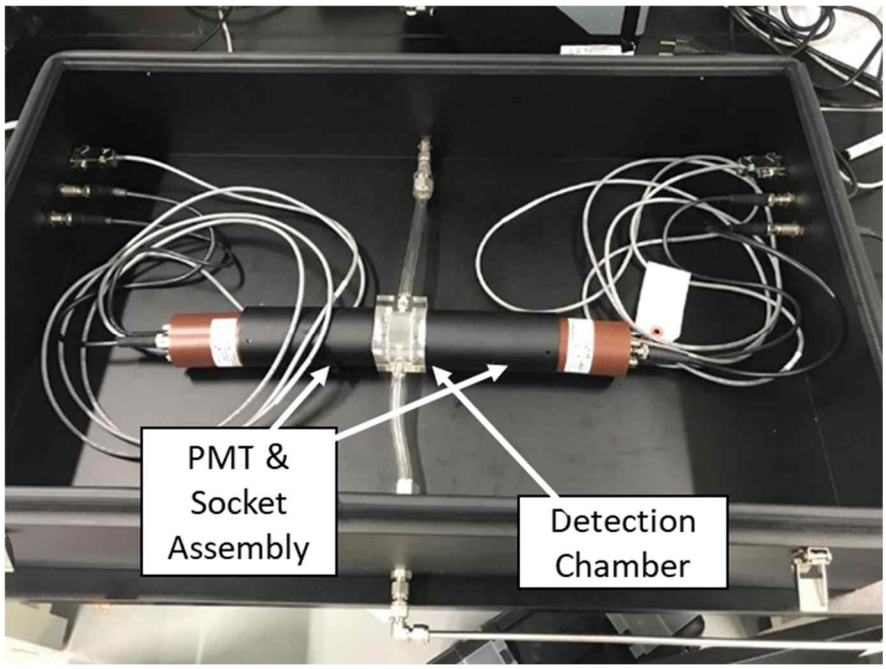

Fig. 3-3. Picture of the preliminary tritium gas detector using plastic scintillator

Two experiments were carried out to characterize electrolysis of tritiated water. The first one was characterization of the fractionation factor of the PEM-based electrolysis cell. Tritiated water samples with knowing concentration were prepared and measured using LSC. The fractionation factor of the tritiated water from the low to high concentration should be constant to use the proposed method. If the fractionation factor were not same nor linear, it is difficult to estimate the tritium concentration in the

original aqueous form. Detailed experiment conditions for the characterization of the fractionation factor were as follows:

- Six spiked water samples were prepared for the electrolysis technique to characterize the fractionation factor and verify the linearity of the tritium concentration in the gaseous sample.
- The tritium concentrations for the liquid samples were 156±3 (S1), 552±11 (S2), 912±19 (S3), 1,296±26 (S4), 1,710±35 (S5), and 2173±44 (S6) kBq L^{-1}.
- The concentrations of these sources were estimated by using a well-calibrated LSC. Each liquid sample was electrolyzed, and the produced tritiated hydrogen gas was collected into a gas sampling bag with a capacity of 3 L.
- The tritium concentrations of the collected samples were measured by using an ionization chamber-based tritium monitor (β-ionix, Premium Analyse).

The second one was continuous measurement test. The experiment was a emulation of practical application in field. A large amount of sample with knowing concentration was prepared and electrolyzed. The produced gas was measured with a given interval. Detailed experiment steps and conditions for the continuous measurement test were as follows:

- 1 L of 7,500 kBq L^{-1} of each sample was prepared for subsequent continuous measurement experiments.
- 1 L of deionized water was initially electrolyzed and detected for 15 minutes, before and 1 ml of the 7.5 MBq ml^{-1} tritium standard source was introduced to the deionized water.
- After one hour of measurement, entire flow path was washed at least 6 times using deionized water, and the measurement was continued.

By evaluating the specific detection efficiency, capability of tritium detection was confirmed and its performance was compared with other previous studies.

The specific detection efficiency was defined as a parameter of the intrinsic detection performance for the plastic scintillator. This parameter is utilized to confirm that the developed detector shows similar

levels of detection efficiency compared with other existing plastic scintillator-based detectors. Singh's work reports that the specific detection efficiency for gaseous tritium was 9.01×10^{-9} cps (Bq L^{-1} $cm^{2})^{-1}$ [19]. The estimated detection specific detection efficiency will be compared with this value. The specific detection efficiency (ε_{area})—efficiency per unit area of the plastic scintillator— is defined as shown in Eq. (2).

$$\varepsilon_{area}\left[\frac{cps}{\frac{Bq}{L}\times cm^2}\right] = \frac{CR}{T_{liquid}\times A} \tag{3.3}$$

where CR and A are the net counting rate recorded by the plastic scintillator, and the surface area of the plastic scintillator, respectively. Detection efficiency was estimated using Eq. (1.3);

$$\varepsilon = \frac{CR}{T_{gas}\times V} \tag{3.4}$$

3.4 Results and Discussion

Fig. 3-4 shows the calibration curve (or line) for liquid water and gaseous tritium concentrations that were used to characterize the electrolysis power of the PEM cell. The relationship between concentration of the tritiated water and gaseous tritium was linear, having a correlation coefficient R^2 value of 0.994. It is important to highlight that the linearity of the tritium concentration of the electrolyzed hydrogen gas and R^2 coefficient ≅ 1 corresponds to reaching minimal errors, as a result of employing the electrolysis method as a pretreatment method. Additionally, the slope of this line represents the electrolysis-based liquid to-gas conversion factor (C_e) as presented in the "Theory" part, and was estimated as being of 0.1362±0.005 [(kBq m^{-3})gas/(kBq L^{-1})liquid]. Solving the Eq. (3.2) yielded an estimated fractionation factor of 5.41±0.20, whereas Soreefan and Deval reported the value of 6.6±0.7 [29]. The relative error was 3.7% while Soreefan's work shows the relative error of 10.6%.

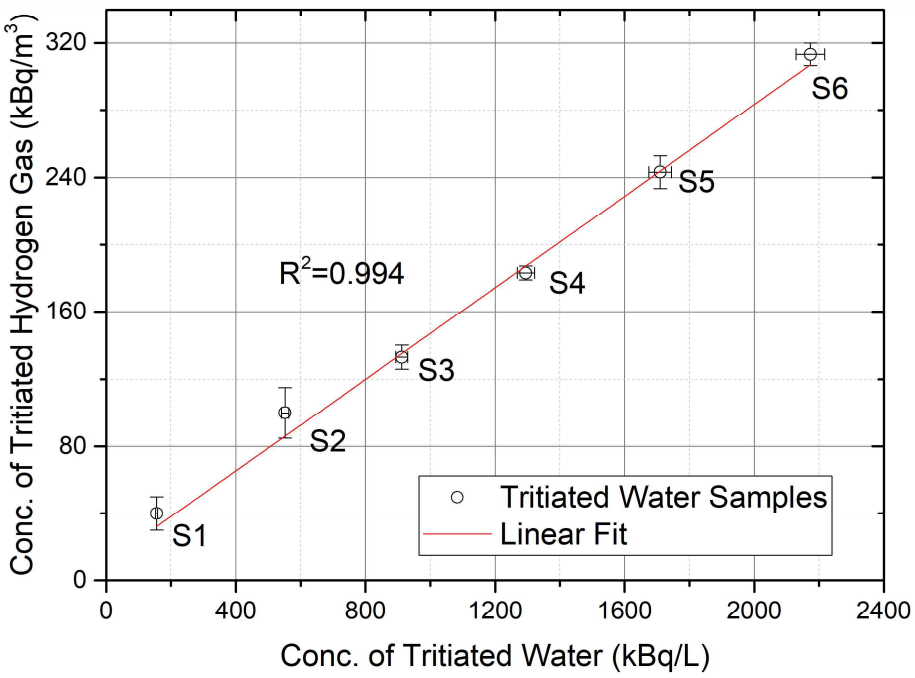

Fig. 3-4. Calibration curve for liquid and gaseous tritium concentrations that was used to characterize the electrolysis of the PEM cell

There are two main reasons to explain why a different value was obtained. One is the difference in the estimation methods. In the work of Soreefan and Devol, the volume was calculated as based on the volume before and after the water was electrolyzed, whereas in this study, water samples with various tritium concentrations were used to derive the relationship between the concentrations of liquid and gas, which was used to estimate the factor. Furthermore, Soreefan and Devol's work may contain volume measurement errors; however, in this study, the error was minimized by using an LSC to perform radioactivity analysis. Secondly, there were differences in the experimental condition (e.g., manufacturer of the PEM cell stack, length and material of flow path, with or without pump for the PEM cell). For these reasons, it is not appropriate to compare direct numerical differences between two studies. Both electrolysis cells showed similar levels of fractionation factor, and the evaluation method used in this study can be used with lower relative error should be focused. If the system is reproduced, the fractionation factor must be evaluated before operation.

Tritium gasification was characterized according to the temperature. In Fig. 3-5, measured counting rate according to the measurement time is displayed along with the temperature of the tritiated water sample. The square markers indicate the instantaneous counting rate, and the solid line, the temperature. The experiment was carried out continuously for 220 min. The counting rate increased as the temperature increased. This implies that more tritium was electrolyzed at higher temperatures for the same concentration of tritiated water. The tritium concentrations measured by the tritium monitor were 90, 130, 190, and 250 kBq/m^3 at temperatures of 30, 50, 70, and 90 ℃, respectively. The corresponding fractionation factors were estimated as 8.90 ± 0.38, 6.23 ± 0.49, 4.26 ± 0.23, and 3.24 ± 0.14 as described in Table 3-1. The fractionation factor fell as the temperature rose. The temperature and counting rate accorded with each other. As a comparison with a study of characterizing tritium enrichment factor in terms of temperature, which reported that the enrichment factor went down as the temperature got higher, it showed a good agreement with this result [42].

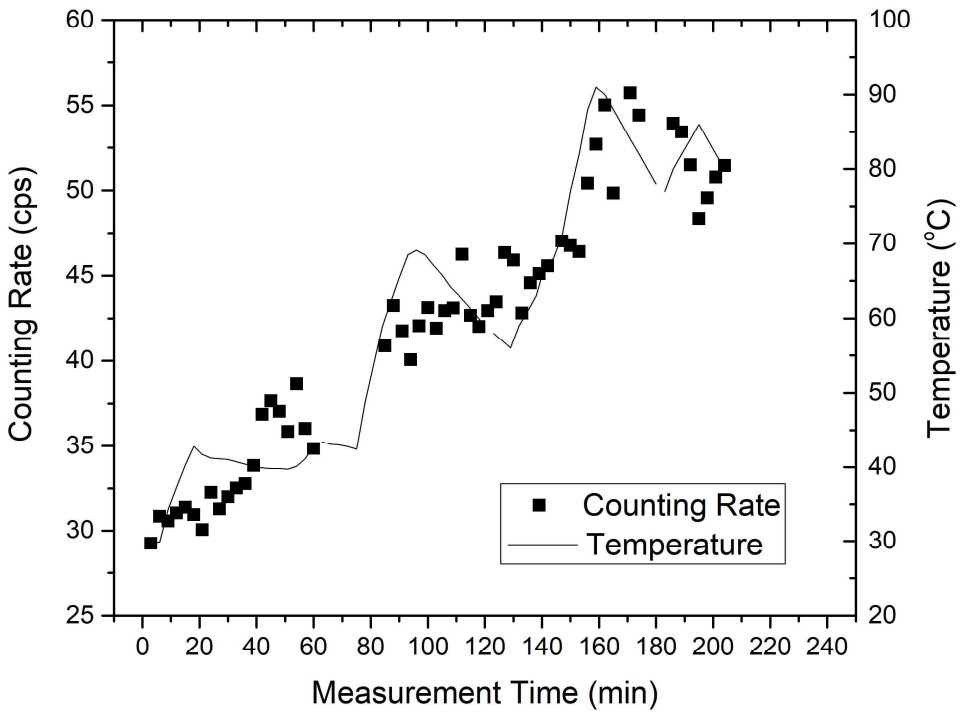

Fig. 3-5. Measured counting rate and the temperature of the tritiated water sample according to the measurement time

Table 3-1. Estimated fractionation factors according to the temperatures

Temperature (℃)	Fractionation factor
30	8.90 ± 0.38
50	6.23 ± 0.49
70	4.26 ± 0.23
90	3.24 ± 0.14

The estimated fractionation factors were quite different from those derived by previous studies. This difference was attributed to the different kinds of electrolysis cells used in those studies. Many past works observed that the electrode material is the primary determinant of the fractionation factor [43-45]. However, the temperature determines the fractionation factor as well, and these variables can be modified suitably to obtain a lower MDA. Thus, practically, the sampled water can change the temperature; if the temperature of the water sample in the system can be monitored and the fractionation factor is applied as a dynamic parameter, it will be possible to monitor the tritium concentration in the water more effectively and accurately

Table 3-2 represents the parameters used in the first experiment using single channel detection chamber, and the estimated detection efficiency, specific detection efficiency and the MDAs obtained on the monitor system. The detection efficiency was estimated using Eq. (4). The specific detection efficiency was estimated as 1.16×10^{-8} cps (Bq L^{-1} $cm^2)^{-1}$, and was improved by 29% relative to the value of 9.01×10^{-9} cps (Bq L^{-1} $cm^2)^{-1}$ obtained by Singh et al [19].

Table 3-2. Parameters used in the experiments and the estimated detection efficiency and specific detection efficiency

Parameters	Values
Background Counting Rate (cps)	3.7±0.06
Net Counting Rate (cps)	1.7±0.02
Tritium Concentration (kBq m^{-3})	1,020±51
Volume of the chamber (m^3)	3.93×10^{-5}
Tritium Activity in Chamber (Bq)	40.1±2.0
Detection Efficiency of the Chamber (%)	4.25±0.22
Specific detection efficiency (cps (Bq L^{-1} cm^2)$^{-1}$)	1.16×10^{-8}
MDA for gaseous tritium (kBq/m^3)	89
MDA for liquid tritium (kBq/L)	655

As Fig. 3-6 shows, the maximum counting rate of the tritiated water sample (322 cpm) was significantly higher than that of the deionized water control (240 cpm). Approximately 45 minutes were required for the counting rate to reach a steady state. This time duration includes the time required for the tritium to mix with the existing deionized water in the sample container, and the time required for the hydrogen gas produced after electrolysis to reach the detection chamber. It is undesirable to apply negative pressure by using a pump, as this may damage the electrolytic cell. Furthermore, if the amount of generated hydrogen gas can be changed by adjusting the current, the desired response time can be achieved. The counting rate after 45 minutes was slightly increased because the tritiated water was enriched during electrolysis. The increase was within the range of error and increase of tritium concentration in the sample container was possible due to enrichment by electrolysis. The water in the sample container was overflowed from the anode to the cathode during electrolysis even more than the decomposition rate. Because of this, the amount of water remaining in the sample container was small and tritium enrichment was accelerated. In practical use, the water sample will be continuously supplied

to the sample container and will not have a significant effect because the sample container always contains a large amount of sample.

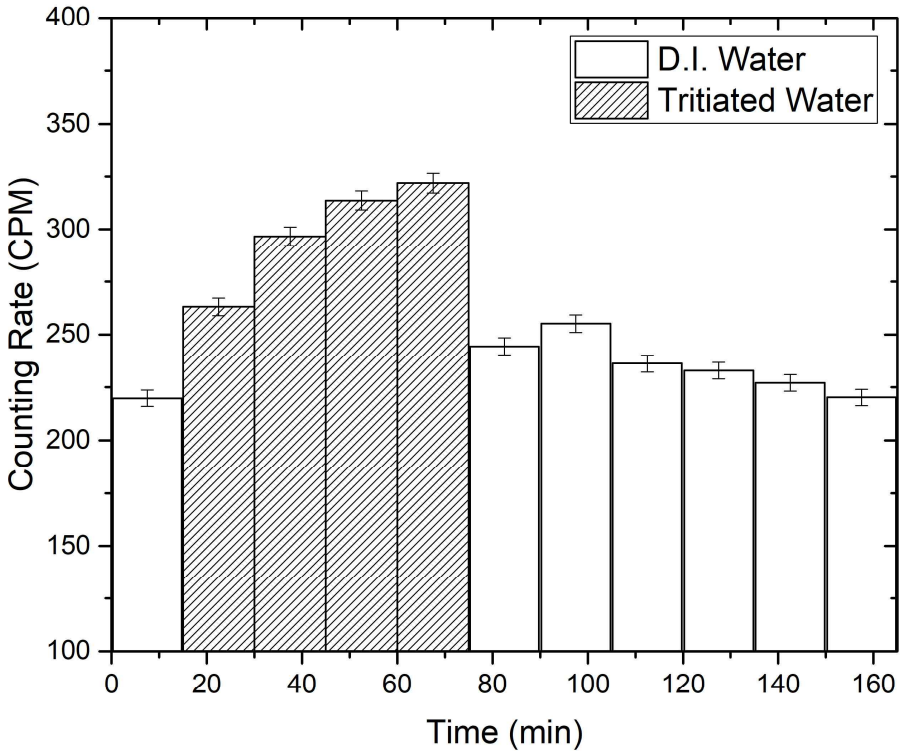

Fig. 3-6. Results of continuous measurement of the counting rate

The MDA for the liquid sample was estimated as 655 kBq L^{-1} under the condition of a measurement time of 60 minutes. Although there are currently no commercially available on-line continuous tritium monitors, the detection limits of the monitor developed in this study was compared to various commercially available models. The MDA of a commercially available off-line real-time tritium monitor (SSS-33M81, technical-associates) was 740 Bq L^{-1} at the background counting time of 24 hours, whereas that of the proposed system was 133 kBq L^{-1}at the same counting time. The response time when a sudden high-activity contamination occurred was relatively short (~45 min). Sudden changes can be detected if they are installed at a point where there is a potential for tritium leaks, at the drain of the nuclear facilities. In addition, unmanned long-term autonomous operation is possible. In general,

there are some differences between the products, deionizing filter and PEM-cell can be used for tens of thousands of hours unless sea water is used [46].

3.5 Computational Calculation of Water Supply System

Configuration of the electrolysis system was drawn and tested by computer-aided design and engineering program. The water sample supply system is included in the electrolysis system. The water supply system was designed before buildup of the experimental setup and its hydraulic and thermal properties were calculated. Fig. 3-7 shows the 3D design of the water supply system. The material of flow lines, joints and containers were set by stainless steel 316L and of connecting tubes for pump and electrolysis cell were set by silicon rubber. The pump and electrolysis cell were expressed as bulk parts without functional details. The outer diameter of the flow line was 6.35 mm and thickness of 0.889 mm which corresponds to the geometry of typical 1/4-inch stainless steel tube. Because it is unnatural to connect directly by welding with a 1/4-inch tube in the container, the 1-inch tube was welded to the sample container and connected to the 1/4-inch tube through two steps of reducing connectors.

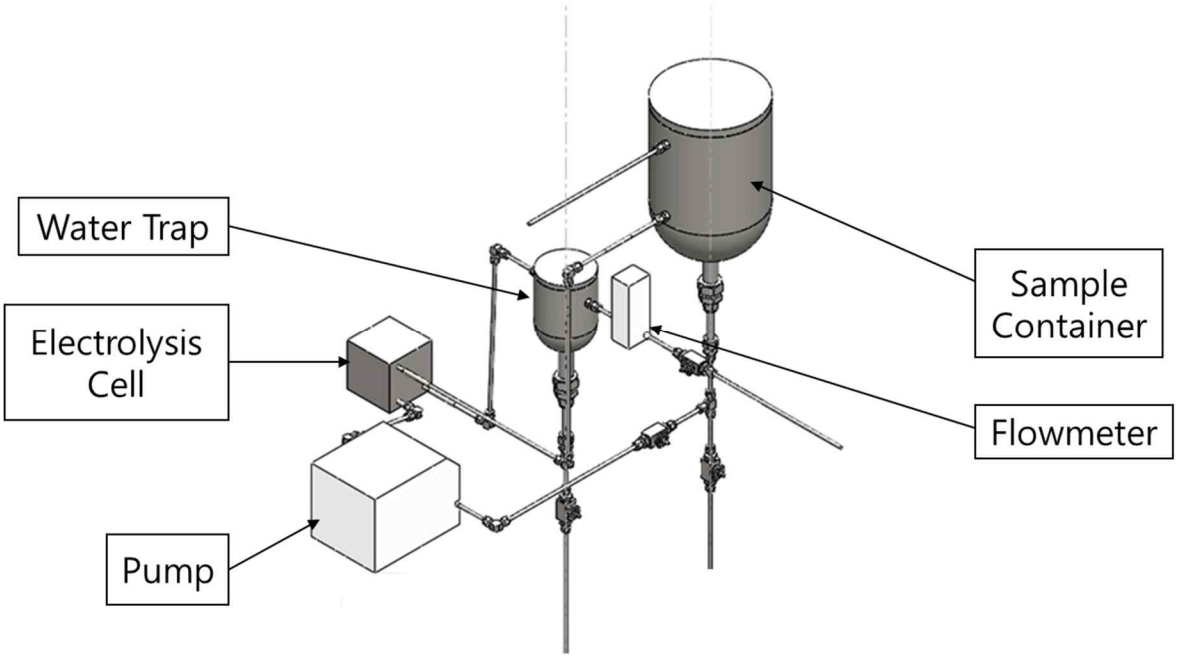

Fig. 3-7. 3D design of the water supply system

The purpose of this simulation is to characterize the difference in temperature of water in the sample container and the electrolysis cell while transporting through the flow channel. Assuming that the cell generates heat of 130 W, the flow rate was set to 1.8 L/min. The mechanical movement of the pump was ignored. The temperature of the water starting from the container was set to 30, 50, 70 and 90 ℃, respectively. The calculation points of the temperature were inlet and outlet of the cell. The operating environmental was set to 25℃ and 1 atm.

Fig. 3-8 shows the temperature distribution in the flow channel with initial temperature of 90 ℃. The temperature of the water was gradually decreasing as it is transported. The volume of the flow channel was estimated by 0.034 L. The total length of flow channel was 2071 mm. The temperature was decreased by 0.017 ℃/mm in average in case of initial temperature of 90 ℃.

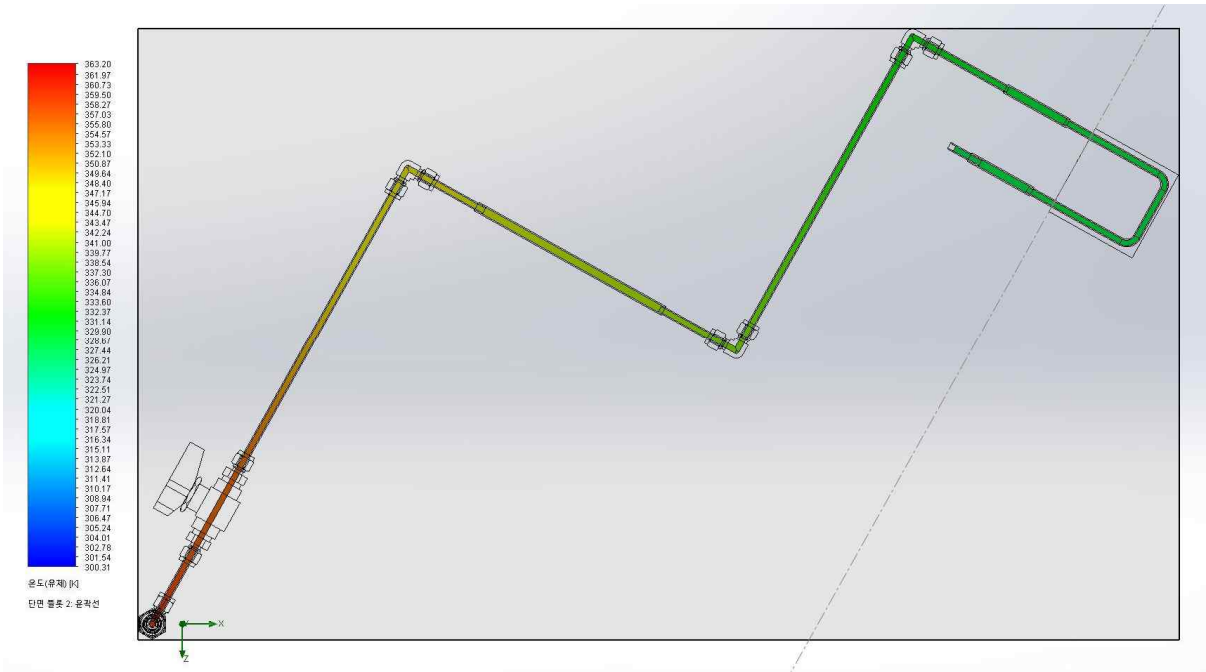

Fig. 3-8. temperature distribution in the flow channel with initial temperature of 90 ℃

Table 3-3 presents the simulated temperature of the water according to the initial temperature. The temperature at the inlet of electrolysis cell were 27.44, 37.07, 46.98 and 55.61 ℃ when the initial

temperature of 30, 50, 70 and 90 ℃, respectively. The temperatures were significantly decreased. The temperatures at the outlet of the electrolysis cell were decreased comparing with that at the inlet. Because the flow channel inside the electrolysis cell was simplified, it was suggested that the heat generated in the electrolysis cell was transferred differently from the actual situation.

Table 3-3. Simulated temperature of the water at the inlet and outlet of the electrolysis cell

Initial Temperature (℃)	Temperature at Inlet of Electrolysis Cell (℃)	Temperature at Outlet of Electrolysis Cell (℃)
30	27.44	27.21
50	37.07	36.25
70	46.98	46.44
90	55.61	55.05

Because the 1/4-inch stainless steel tube could be used for heat exchange and the flow path was considerably long, the temperature decrement was significant. For practical usage, it is desirable to shorten the length of the flow path, and temperature sensor should be placed in the electrolysis cell to measure the temperature of the electrolyzed water, precisely. Additionally, it can be considered to insulate the tubes and the electrolysis cell to reduce power consumption for heating the water.

3.6 Summary

The electrolysis characteristics for the tritiated water was investigated. The novel method of estimating the fractionation factor was suggested. The tritiated water was electrolyzed from low concentration to high concentration and concentrations of the tritiated gas generated from the electrolysis was linear with R^2 value of 0.994. The fractionation factor was successfully estimated with about three times lower relative errors. By connecting the electrolysis system and preliminary detector, simple test for continuous monitoring of tritium in water was conducted. The system included a PEM-based electrolysis setup and a simply designed single-channel plastic scintillator chamber for low-energy beta ray measurement. The proposed tritium detection method yielded a specific detection efficiency that is 29% higher than that reported by previous authors. Though the detection efficiency was too low and the volume of the chamber too small, it was confirmed that the continuous monitoring of high concentration of tritiated water was possible. This system is expected to be applied as a tritium-in-water monitor to investigate a leakage in nuclear facilities and check the status of tritium production facilities. However, it is necessary to improve the detection part in order to monitor the tritium at a lower concentration.

Chapter IV. Multi-channel Plastic Scintillator Tritium Detection Chamber and Performance Test

4.1 Advantage of Multi-channel Detector

The plastic scintillator is physio-chemically stable, and its optical characteristic is not vulnerable to the environmental condition. Moreover, it is advantageous for beta ray measurements because of their low atomic number and small backscattering or Bremsstrahlung effects. Therefore, beta ray measurement using plastic scintillators is advantageous if the detection efficiency is increased. A disadvantage of the plastic scintillator for measurement of a beta ray is its low detection efficiency because the beta ray should fly to the scintillator and interact before it loses its all energy. If the size of the detection chamber is increased to increase the volume of the detectable gas, the beta rays emitted from a distant location than the beta rays' range will lose all energy in the gas inside the chamber, which will lead to a decrease in detection efficiency. Therefore, it is important to improve both detection efficiency and volume of the chamber with proper design for measurement of tritium beta rays with short range.

In this chapter, a design of plastic scintillator-based multi-channel tritium gas counting chamber was proposed. Thin planar plastic scintillators are arranged to form a number of gas-flow channels. The spacing between the scintillators is small enough to detect beta rays with short range. Design and evaluation of the detection efficiency was carried out using Monte Carlo N-Particle 6 (MCNP6) code. Various design parameters were applied to evaluate the performance of various detector designs through particle transport simulation. Additionally, optimization of the coincidence circuit composed in chapter 2 was carried out. The outputs according to the parameters of the circuit depends on the design method of the detector due to changes in optical transportation efficiency. Therefore, the circuit parameter was optimized by applying the detection chamber that had been designed and manufactured in this chapter.

The performance was evaluated by defining a figure of merit that can determine the minimum detectable activity (MDA) which is directly related to the performance of the detection system. The proposed novel design method for a gaseous tritium detector and the simulation method used in this study are expected to be used in another tritium detector design study.

4.2 Calculation of MDA and Definition of FOM

When the number of channels is increased, the number of plastic scintillators is also increased, and the volume of the channel is reduced by that amount. The detection efficiency is increased by exponential decay. The number of channels is related to the gap (or thickness of the hydrogen gas layer) between the source position and the plastic scintillator. When the gap between two scintillators is decreased, the length of the attenuation in the hydrogen gas medium is decreased. The full physical model for calculating the beta ray detection efficiency would be more complex. However, it is sufficient to explain the detection efficiency curve pertaining to the number of channels. Therefore, the expected mathematical model and the expected counting rate can be expressed by Eq. (4.1) and Eq. (4.2), respectively:

$$y = A_0(1 - e^{-\mu x})(A_1 x + A_2) + C \tag{4.1}$$

$$CR = \varepsilon \cdot M \cdot t \tag{4.2}$$

where A_0, A_1, A_2, and C are the parameters for the mathematical model and CR, ε, M, and t are counting rate, detection efficiency, volume of the chamber, and concentration of the tritiated hydrogen gas, respectively. The simulated results were fitted based on Eq. (1) to clarify the accordance with the physical model. For MDA estimation, the general Currie expression was used with modification, which is suitable for the developed system. The MDA of each detection chamber was simply calculated using Eq. (4.3) which is based on the general Currie's MDA expression.

$$\mathrm{MDA}\left[\frac{\mathrm{Bq}}{m^3}\right] = \frac{2.71 + 4.65\sqrt{C_B}}{\varepsilon \cdot M \cdot t} \tag{4.3}$$

The C_B is a background count that was obtained from the preliminary detection system. The MDA calculated in this part is just a reference value for predicting the detector performance. The ε and C_B

were expected to be different from the simulated and experimental results. The detailed calculation of MDA of the developed system will be further discussed in chapter 5.

The electronic signal acceptance condition was characterized. The detector type used in the study was plastic scintillator-based detector. The plastic scintillators generate light signal by interacting with the beta ray followed by the decay of tritium. In case of tritium, the generated light signal is very weak because the energy of the beta ray is very low. Therefore, amplification degree—also known as gain—and low discrimination level (LDL) are critical in signal counting. The number of the desired signal is increased when the gain is increased, the noise signal is also amplified. However, the counting rate of background signals due to dark currents caused by thermal diffusion can be increased, resulting in an increment in MDA. To avoid the overflow of the noise signal, proper gain and LDL should be selected. To obtain an optimal balance between the detection efficiency and background counting rate, the figure of merit (FOM) was defined as in Eq. (4.4).

$$\mathrm{FOM} = \frac{\varepsilon^2}{C_B} \tag{4.4}$$

where ε and C_B are the detection efficiency and background counts, respectively.

4.3 Computational Simulation

When using the plastic scintillator as a gaseous radioactivity detector, the most important point is detection efficiency. Because the plastic scintillator, unlike gas-filled detectors, cannot record all of the beta rays generated in the chamber, the gap between scintillators should be decreased to maximize detection efficiency. However, as the gap is made smaller, the volume of the gaseous sample also becomes smaller. Therefore, the trade-off between detection efficiency and sample volume should be optimized.

Fig. 4-1 shows the cross-sectional view of the detection chamber and its design parameters. The design parameters are the width (*W*), depth (*D*), and height (*H*) of the chamber, thickness of the outer acrylic structure (*T*), thickness of the plastic scintillators (*t*), and number of channels (*n*). To apply the commercial 5-inch (127-mm) photomultiplier tube (PMT), the D and *H* were fixed at $127/\sqrt{2} = 89.8$ mm. PMTs were optically coupled with x-axis direction when experiment was carried out. Therefore, if the scintillators are bigger than the window size of the PMT, photons are escaped, and optical loss occur. The *T* was fixed as 5 mm by considering the structural strength. Thin slots were processed on the two facing sides of the acrylic chamber and the plastic scintillators were inserted. Both sides were open to contact the plastic scintillators and PMT windows. The values of 0.5, 1.0, 1.5, and 2.0 mm were selected as the values for *t* that could actually be processed. The *n* values are 1, 2, 4, 8, 12,⋯, increasing by 4 channels.

W was set by 79.8 mm, which corresponds to the value of $D - 2t$ $(89.8 - 2 \times 5)$. W can be increased to effectively enlarge the volume of the detection chamber. Before increasing W, light transmission rate and structural stability of the thin scintillator should be considered. Light transmission rate determines the signal amplitude. As the system includes coincidence system, amplitudes of light signals arriving at both PMTs are preferred to be similar. If one signal is rejected due to the cut-off amplitude in signal processing, the other one would be not recorded or be an outlier point from the ROI. The light attenuation coefficient for 5, 10, and 20 mm-thick plastic scintillators were 190, 210, and 275 cm. Though the manufacturer of the plastic scintillator does not supply information of light attenuation

coefficient for the thickness of 1 mm or less, it is expected to be much shorter. When using the value of 190 cm, 20 cm of length can transmit 90% of the light. From this, W longer than 200 mm is not desirable. For the structural stability, bending of the scintillators is expected when W is much longer than the D. In this aspect, flexural modulus (E_{bend}) has been quoted to predict the deformation of material which is supported by two end points and forced by a point in the center [47, 48]. The flexural modulus is defined as:

$$E_{bend} = \frac{W^3 F}{4Dt^3 d} \tag{4.5}$$

where d is the deflection due to the loaded force (F) and other variables are substituted as design parameters used in this chapter. The flexural modulus value is 2920 MPa for 50 mm-thick plastic scintillator provided by the manufacturer (Saint-Gobain Crystal). Calculated deflections are listed in Table 4-1.

Table 4-1. Calculated deflection of scintillator according to the thickness and width of scintillator

Thickness of scintillator (mm)	Width of the scintillator (mm)	Deflection of scintillator (d =ΔW/W)
0.5	79.8	0.14
	140	0.78
	200	2.3
1	79.8	0.036
	140	0.19
	200	0.56
2	79.8	0.0090
	140	0.049
	200	0.14

Note that the flexural modulus value for the thin plastic scintillator and failure point of deflection are not provided, the calculated vales are utilized to predict the stiffness of the scintillator according to the thickness and width of the scintillator. When the thickness of the scintillator is 0.5 mm, deflection is 0.14 though it has shape of square. Therefore, it would be structurally unstable and light transmission rate is expected to be decrease due to bending. When thickness is 1 mm, deflection is 0.036 for the square shape. The value enough low to be handle. However, when it has larger width, the deflection increases drastically. When thickness is 2 mm, deflection is 0.0090 for the square shape, and 0.049 for width of 140 mm. Increasing the width and increasing the volume of the chamber can be beneficial based on its structural stability, but the volume of gas inside the chamber, which decreases with increasing the number of channels, is also large, thus, it can be trade-off. For these reasons, it is reasonable for the plastic scintillator to have a square shape with a W of 79.8 mm.

The geometry of the detection chamber was the same as that shown in Fig. 1. The gas channel (blue color in Fig. 1) was filled with hydrogen gas at a density of 8.99×10^{-5} g/cm^3. The isotopic fraction of tritium was ignored because the number of tritium atoms in the tritiated hydrogen gas with order of a few kBq/m^3 is ignorable. The acrylic structure (green color in Fig. 1) was poly-methyl methacrylate (PMMA, $(C_5O_2H_8)_n$) with a density of 1.18 g/cm^3. The plastic scintillator (red color in Fig. 1) was carbon hydrate with a C/H ratio of 1.103 and density of 1.032 g/cm^3.

The input source of beta ray from tritium was extracted from the 'Radiological Toolbox' developed by Oak Ridge National Laboratory [35]. The input values were modified in a way suitable for the MCNP6 source input card. One hundred energy bins were used to emulate a continuous-like beta ray source. The source position was carefully defined to be only in the gas channel and not positioned onto the plastic scintillator. The tritiated hydrogen gas was assumed to be homogeneous. The F8 tally was used to record the energy deposited in the plastic scintillator. Deposited energy less than 1 keV was rejected in the detection efficiency calculation. To make the relative error less than 0.5%, 10 million particles were transported.

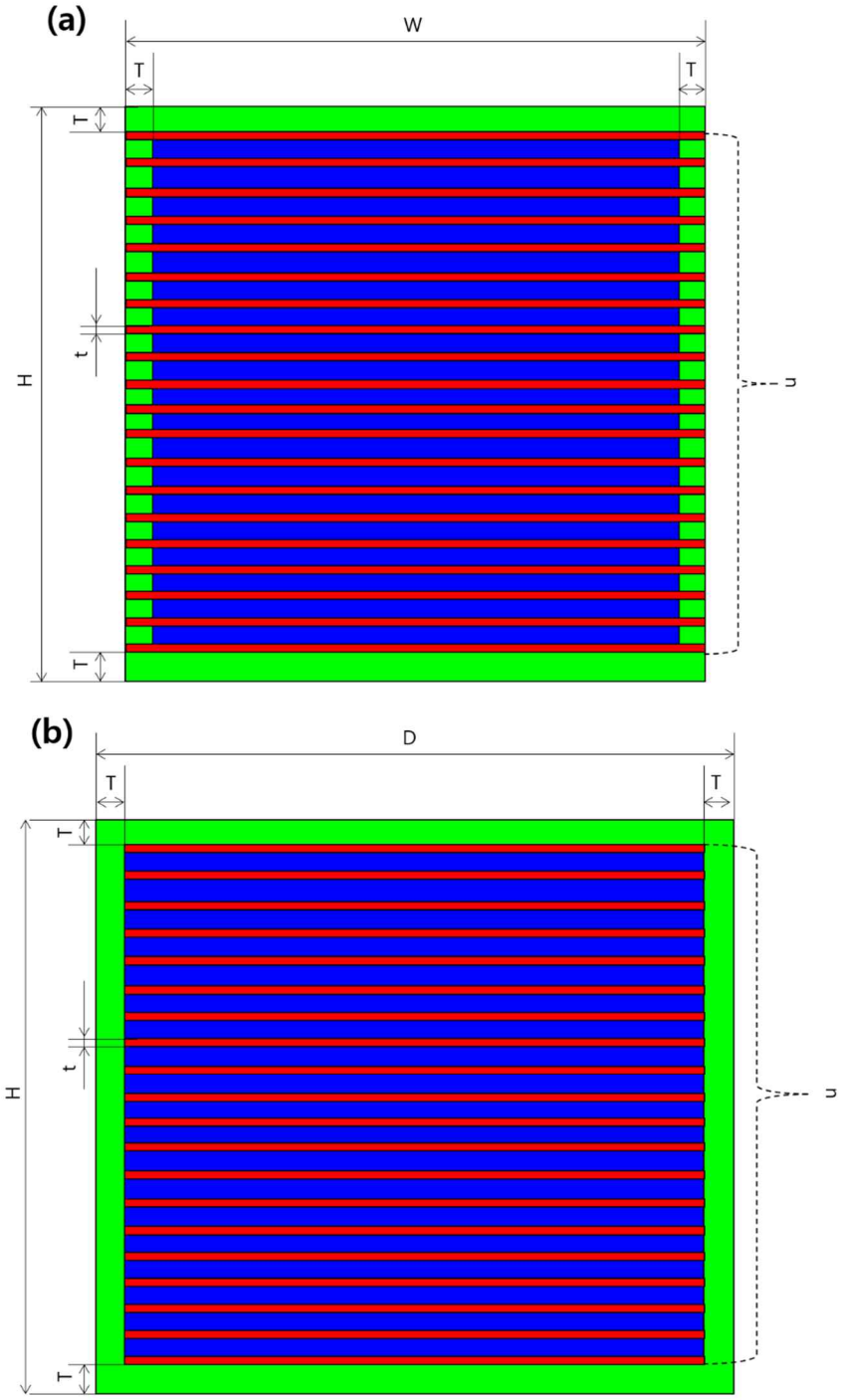

Fig. 4-1. Cross-sectional view of the plastic scintillator-based detection chamber perpendicular to the (a) y-axis and (b) x-axis, and its design parameters: *D* (depth of the chamber), *W* (width of the chamber), *H* (height of the chamber), *T* (thickness of acrylic structure), *t* (thickness of the plastic scintillators), and *n* (number of scintillator slots).

4.4 Experimental Setup

Multi-channel detection chambers were fabricated to verify the simulation result. Fig. 4-2 shows the 3D design of the multi-channel scintillation chamber. The width, height, and thickness of the acrylic structure were the same as in the simulation. The thickness of the plastic scintillator (Epic-Crystal Ltd.) was 1.0 mm. The plastic scintillators were fixed using optical cement (BC-600, Saint-Gobain Crystals). Due to processing limitations of an acrylic structure, a 12-channel detection chamber was used as a representative of multi-channel detection chamber. Although only one type of multi-channel detection chamber was tested, it is sufficient to show the improvement in the detection efficiency because it is the maximum number of channels that can practically maximize the detection efficiency.

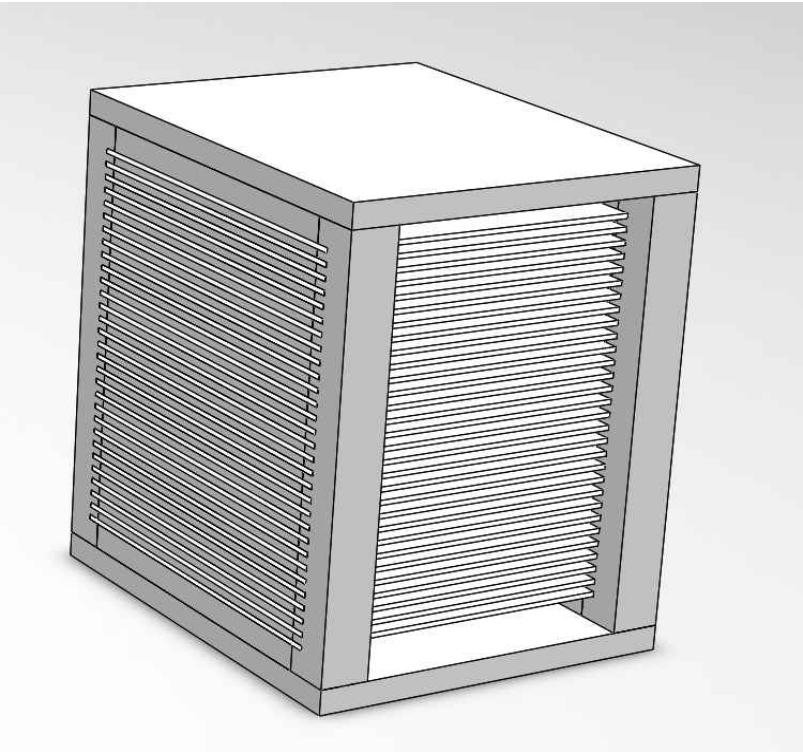

Fig. 4-2. 3D design of multi-channel scintillation chamber

Fig. 4-3 shows the fabricated chamber which is coupled with the PMTs and flow path of the electrolysis system. A photomultiplier tube (PMT)-based light detecting system was used to collect and

convert the light signal into the voltage signal. The composition of the coincidence circuit was same that was used in the chapter 2 except for the PMT. The detection chamber was placed between PMTs with window diameter of 127 mm(R877, Hamamtsu Photonics, Japan), and aligned precisely to avoid signal loss. The chamber was made using a 77 × 77 mm^2 planar plastic scintillator (plastic scintillator, Epic Crystal Ltd., China) with a thickness of 1 mm. The volume of the chamber was 424 cm^3. The PMTs were mounted on the PMT sockets with a preamplifier (Model 276, Ortec Inc., USA), and the output signals were amplified using a dual spectroscopy amplifier (Model 855, Ortec Inc., USA). The coincidence technique was adopted by timing a single channel analyzer (Model 511, Ortec Inc., USA) and a time-to-amplitude convertor (TAC) (567, Ortec Inc., USA) to reduce the background counting rate. The time-to-amplitude convertor gives a time difference information and confirm the signals are from the same generated scintillation photon. The information was analyzed using a multi-channel analyser (EASY-MCA-2K, Ortec Inc., USA) and signals only time difference within 500 ns are considered as usable signal.

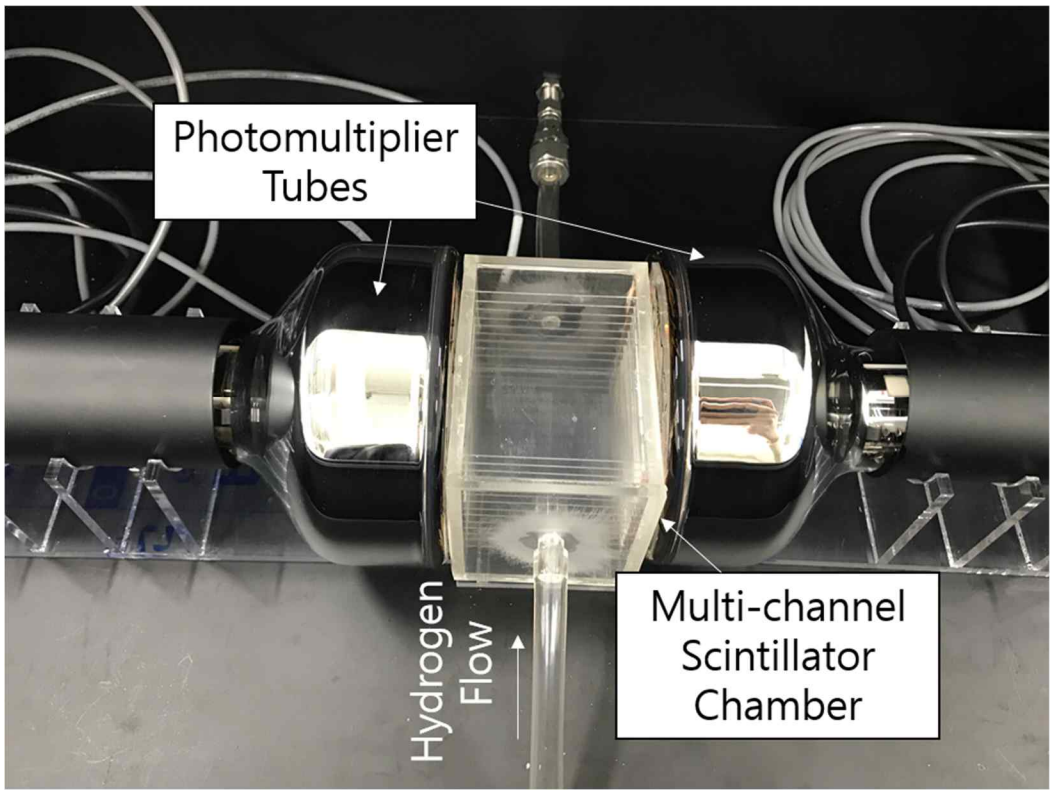

Fig. 4-3. The developed multi-channel scintillation chamber coupled with light detecting apparatus

In the chapter 2, energy calibration as carried out. In chapter 2, the backend channel of the tritium spectrum was 89-th Ch when using the gain of 80. In this experiment, the trade-off between detection efficiency and background counting rate was optimized by increasing the gain to reach the backend of the spectrum to the maximum channel and setting the LDL appropriately. As shown in Table 4-2, tube diameter and gain are different between two models. The diameter is 2.5 times higher and gain is 2.27 times lower for R877. The pulse height depends on the window diameter, gain and light transportation efficiency. By considering the window diameter and gain, the pulse height will be increased 2.75 times. However, in case of using R878, the scintillator was attached to the PMT window parallelly but in case of using R877, it was vertically coupled. Therefore, the light transportation efficiency will be decreased. Considering the refractive index of the plastic scintillator (1.58) and applying the Snell's law, the critical angle is 39.27° [49]. The solid angle at the critical angle was calculated by 0.903π for both upper and lower side directions [50]. Dividing it by 4π, the loss of the photon will be 22.6%. As a result, reflection at the sealed tritium source, it was supposed that the advantage due to the difference in PMT would almost be canceled out, except for increasing of the chamber volume.

Table 4-2. Specification of PMTs. Model R878 vs Model R877

Model	R878	R877
Tube diameter (mm)	51	127
Spectral response range (nm)	300 to 650	300 to 650
Anode to cathode supply voltage (V)	1500	1250
Gain	1.0×10^6	4.4×10^5
Dark current (nA)	5	10
Time response – Rise time (ns)	7	20
Time response – Transition time (ns)	70	115
Time response – FWHM (ns)	N/A	18.5

To optimize the FOM, the LDL was adjusted from 0.6 to 1.4, and two gains were used: 600 and 900. The gains were acquired using both coarse gain and fine gain. The coarse gain was fixed by 100 and fine gain was changed by 6 and 9. Because the time response characteristics were different, ROI was newly set using the same method used in the chapter 2, 2 times of the FWHM for the coincidence spectrum peak.

Tritiated hydrogen gas was prepared by electrolysis of a tritiated water sample. The electrolysis system for producing the tritiated hydrogen gas was same as described in chapter 3. The generated hydrogen gas was transported to the detector box through the hydrogen buffer. The hydrogen buffer was half full of water to transport the produced hydrogen gas stably and collect the overflowed water from the electrolysis cell. The general operating condition was 7 A-18 V, which was supplied by the power supply, and its corresponding hydrogen production rate was 660 mL/min. The tritiated water sample was prepared by diluting a tritium standard source (Eckert & Ziegler). Gaseous samples with concentrations of 832 ± 12 kBq/m^3 was produced and used to estimate the detection efficiency of the single- and multi-channel detection chamber, respectively. The tritium concentration of the gaseous sample was measured by a tritium monitor (β-ionix, Premium Analyse). Tritiated water sample with a concentration of 1 MBq/L was prepared. The sample was electrolyzed and its expected tritium concentration in the produced hydrogen gas was 233.3 ± 69.3 kBq/m^3 when a fractionation factor which was evaluated in the chapter 3 was applied. The produced gas flowed into the developed plastic scintillator-based detection chamber.

The produced tritiated gas was injected into the detection chamber and counted for 5 min. This experiment was repeated three times for each detection chamber. For each repetition, the chamber was rinsed using nitrogen gas (99.9%) for 5 min. The rinsed gas was treated as non-radioactive exhausted gas because the tritium concentration of the gas was lower than the regulatory exemption criterion (40 MBq/m^3) and the gas was sufficiently diluted.

4.5 Results and Discussion

Fig. 4-4 shows the detection efficiency and volume of the chambers with varying number of channels. The volume of the chamber decreased linearly. It was straightforward because the two sides of the channel were the same and only the height was changed. The detection efficiency of the chamber increased with saturation growth. When the thickness of the plastic scintillator was 1.0 mm, the crossing point between detection efficiency and volume of the chamber was $n = 24$. This point is expected to be the maximum counting rate point according to Eq. (2).

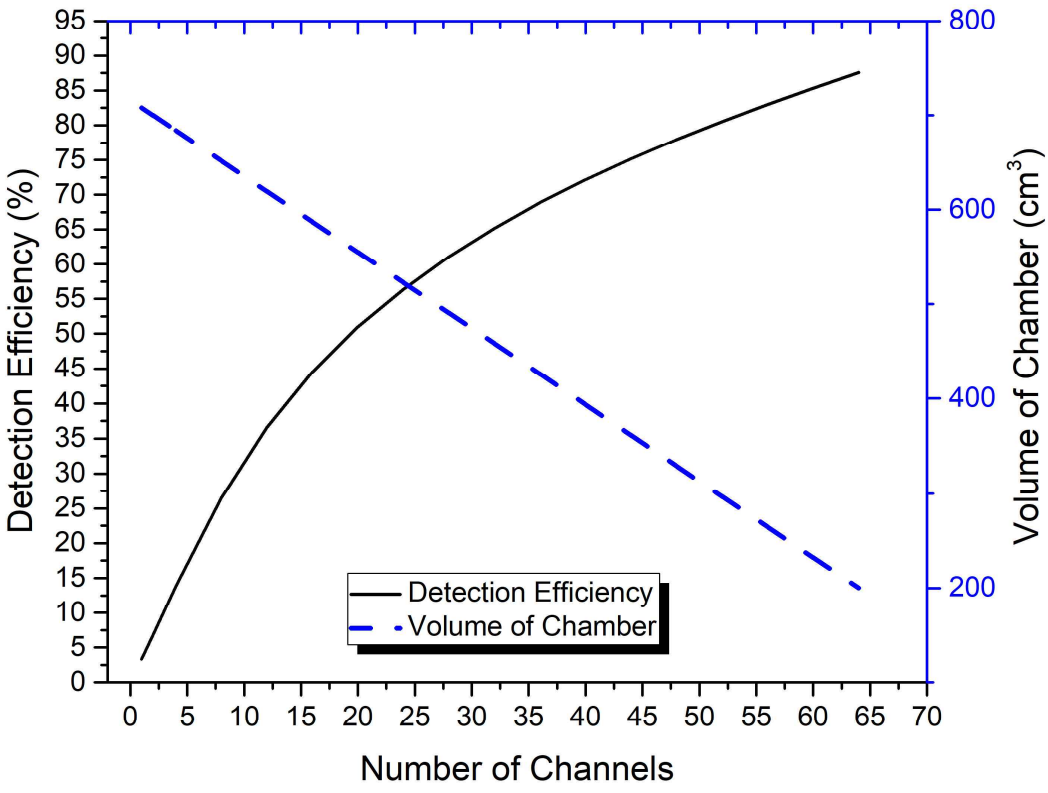

Fig. 4-4. Detection efficiency (solid) and volume of each chamber (dashed) with varying number of channels when the plastic scintillator thickness was 1.0 mm

Fig. 4-5 shows the simulated spectrum data of tritium measurement. Total detection efficiencies according to the different number of channels were 4.7%, 9.6%, 18.8%, 33.8%, 53.7% for 2, 4, 8, 16, 32 channels, respectively. Until 16 channels, the detection efficiency was doubled when the number of channels was doubled. The reason for the increase in detection efficiency is that the beta rays lost in the empty space inside the chamber are measured as a new scintillator is added. As the number of channels increases, scintillators are added by that number, and when the number of channels is doubled, the number of scintillators is doubled, thus the efficiency increases. However, when it reaches about 32 channels, the number of beta rays lost in the empty space is relatively reduced, and the advantage of measuring the lost beta rays decreases even when a scintillator is added in the empty space. Therefore, from 16 Ch to 32 Ch, the detection efficiency was increased 1.59 times though the number of the channel was doubled.

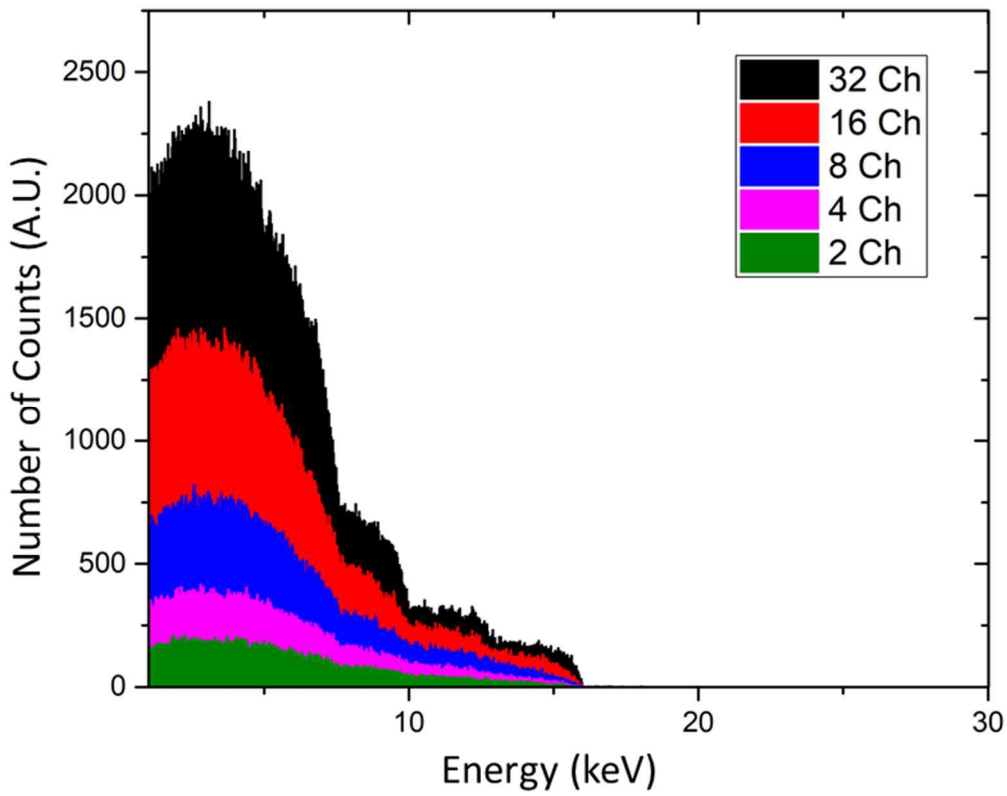

Fig. 4-5. Spectra of tritium measurement simulation with different number of channels

Fig. 4-6 shows the expected counting rate based on the MCNP6 simulation results. It was assumed that 100 kBq/m^3 tritiated hydrogen gas was injected into the detection chamber. The curves fitting each thickness of the plastic scintillator were determined based on Eq. (4.1). The R^2 values for all curves were more than 0.99, which means that this mathematical or physical model is well matched. The local maximum values for the curves were shown at n = 48, n = 28, n = 24, and n = 16, respectively. When the thickness of the plastic scintillator was 0.5 mm, the maximum counting rate was shown. The smallest MDA was shown at the same point. The smallest MDA was estimated as 29.9 kBq/m^3 with a counting time of 30 s, whereas the work of Aoyama et al. showed a value of 37 kBq/m^3 with the same counting time [25]. During MDA estimation, the background counting rate was considered to be same (167 cps) as in the experimental work. As the number of channels is increased, the background counting rate could be increased because the volume of plastic scintillator is increased.

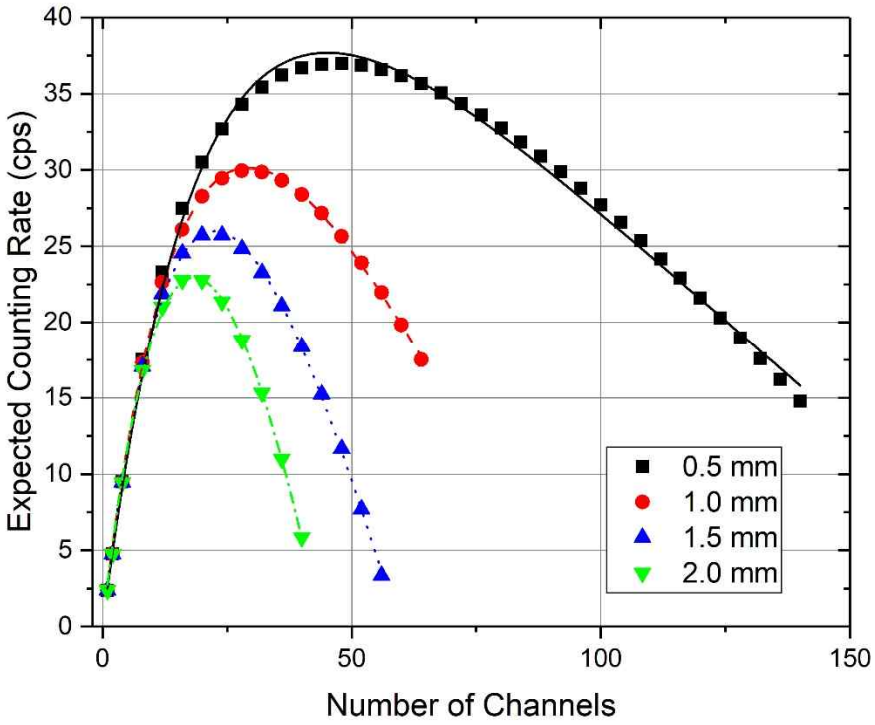

Fig. 4-6. Expected counting rates for different scintillator thicknesses when tritiated hydrogen gas with a concentration of 100 kBq/m^3 is injected into the multi-channel detection chamber

However, that effect is not expected to be significant because the detection efficiency of the plastic scintillator to external gamma or cosmic rays is very low. There was no lead shield to reject external gamma or cosmic rays and thus decrease the background counting rate in the experimental work. If a lead shield were to be added according to the purpose of the use, a lower background counting rate would be obtained, which means that a slightly lower MDA could be expected [19]. In this case, monitoring of tritium in the environmental atmosphere is expected to be possible.

Fig. 4-7 shows the measured counting rates for single-channel and 12-channel tritium detection chambers. Linearity and reproducibility were clearly shown with a low relative error. The experimentally measured result showed that the detection efficiency of the single-channel detection chamber was 1.78 ± 0.04% and that the detection efficiency of the 12-channel chamber was 27.91 ± 0.49%, and relative standard deviations for the detection efficiencies of the chambers were 2.25% and 1.76%, respectively.

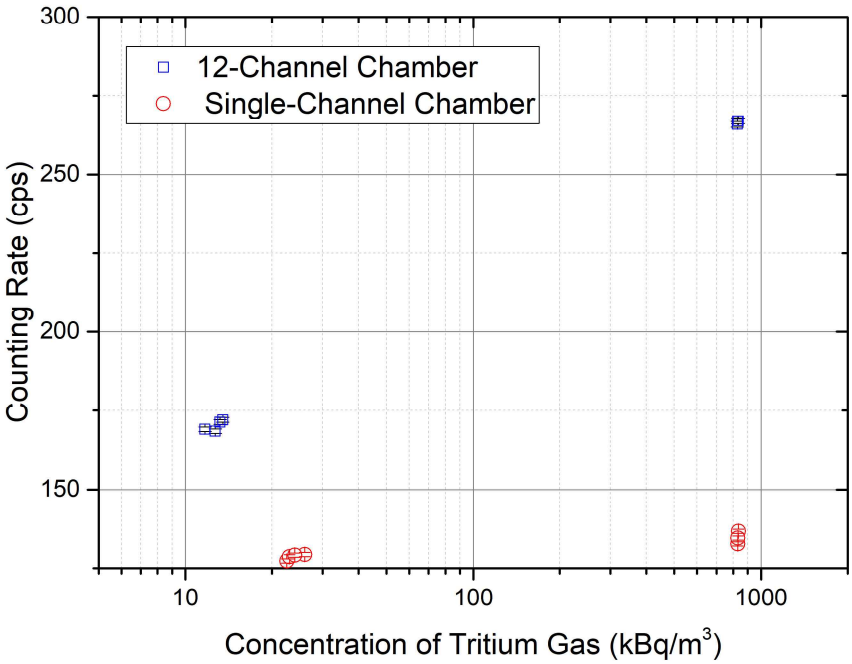

Fig. 4-7. Measured counting rates for the single-channel (circle) and 12-channel (box) tritium detection chambers

The simulated efficiencies of the same chambers were 3.36% and 36.56%, respectively. The experimental work showed lower efficiencies because of the lower level of discrimination (LLD) of the light detecting apparatus and loss during light transportation. In the simulation, the LLD was set as 1 keV and loss during light transportation was ignored. The relative differences of the efficiencies between the simulated and measured work were 47.0% and 24.7%, respectively. The main reason for the difference was thought to be the difference in optical loss during transmission. In the case of the single-channel chamber, the number of scintillators was small, so the size of the cross-sectional area for light transmission to the PMT was small. This implies that the proposed multi-channel type chamber is improved compared with the single-channel type.

For practical application, two things need to be discussed: memory effect and lifetime of the chamber. The hydrogen gas could be adsorbed on the surface of the hydrocarbon due to van der Waals force [51]. However, it is sufficiently weak such that it can be desorbed with a mild mechanical impact, such that the porous carbonate structure can stably store the hydrogen gas [52]. During the experiments carried out in this study, nitrogen gas, with a regulated pressure of 0.3 bar, was used to rinse the detection chamber, and there was no observable memory effect. The developed detection chamber can be operated in a high-level tritiated environment if a ventilation system with proper pressure is adopted.

There was a concern that the optical transmission of the signal produced by the plastic scintillators with thin optical channel would be poor. However, the refractive number of the plastic scintillator was 1.58, where the corresponding critical angle was 39.2°. Because the critical angle for total reflection was less than 45°, it was expected that the light would be transported more in the direction of the thin optical channel than in the normal direction through which light would escape. Although not directly measuring the lifetime, the detection chamber can be used semi-permanently at room temperature unless it is physically damaged. The acrylic structure and plastic scintillator are stable at room temperature, and the optical cement is sufficiently long lasting.

Fig. 4-8 shows the estimated detection efficiency estimated using the Eq. (3.4). The detection efficiency increased when the LDL was decreased in case of fine gas was 6. The maximum detection efficiency was estimated to be 43.0 ± 4.32% when the LDL and fine gain were 0.6 and 6, respectively. However, In case of fine gas was 9, detection efficiency was increased until LDL was lowered to 0.8. When LDL was 0.6, the detection efficiency was decreased drastically. If huge amount of noise signals are input as the LDL is lowered, the noise signal may interrupted to the desired timing signals, and thus the counting rate in the ROI may decrease due to the characteristics of the coincidence circuit. Detection efficiency may increase if the total counting rate rather than ROI is considered, but in that case, the background counting rate was too high and thus it was unsuitable to be used practically.

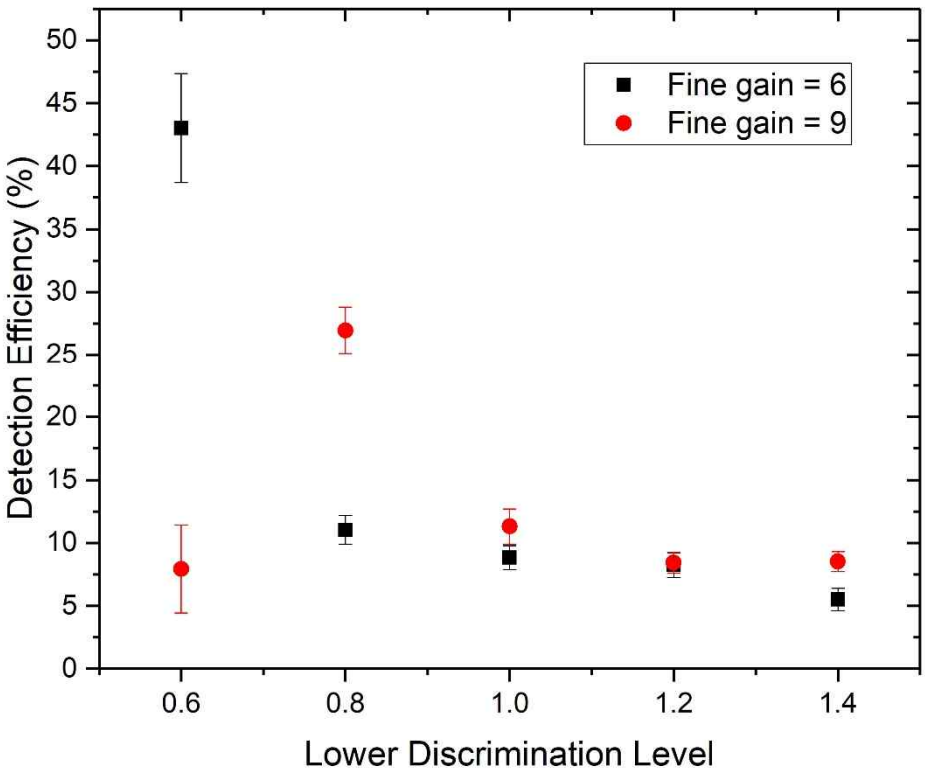

Fig. 4-8. Estimated detection efficiency according to the LDL and fine gain

Fig. 4-9 shows the FOMs evaluated using the Eq. (4.4) according to the LDLs and fine gains. The FOM increased when the LDL decreased and the fine gain was 6. However, if the fine gain was 9, the FOM reached its maximum (0.8) at the LDL and decreased with lower LDLs to 0.6. This was because the background counting rate was very high when the LDL reached a specific threshold. The results also showed that the optimal condition of detection corresponds to the maximum FOM of 0.120, with an LDL and a gain of 0.6 and 600, respectively.

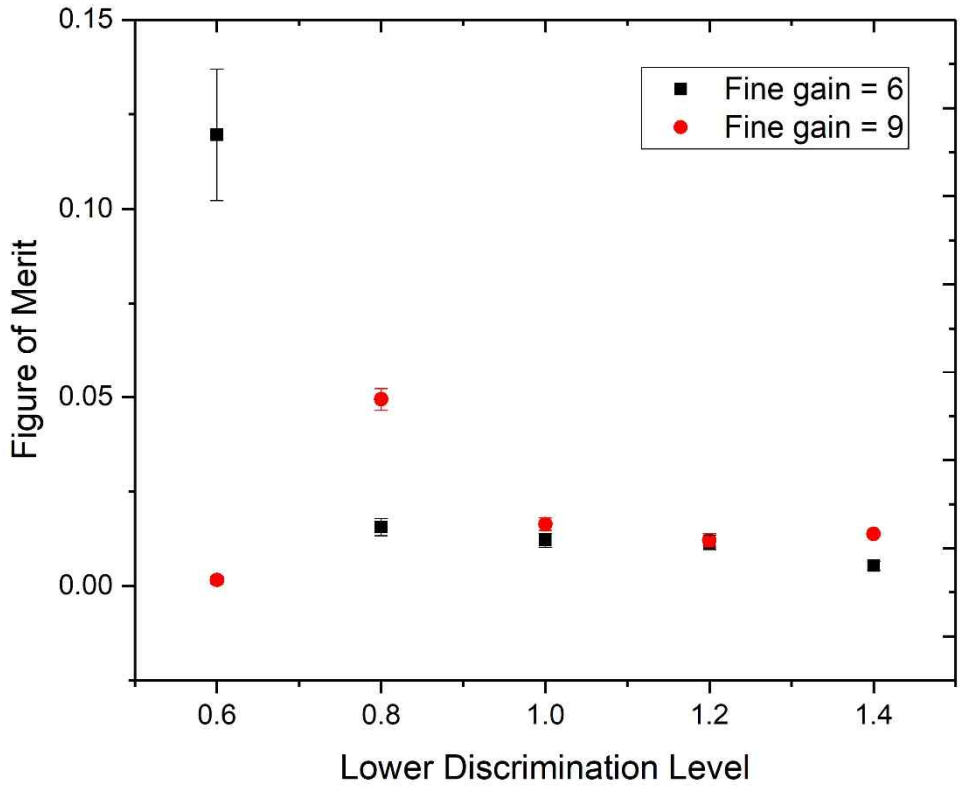

Fig. 4-9. Evaluated figure of merit (FOM) according to the LDL and fine gain

4.6 Summary

A novel design of the plastic scintillator-based multi-channel detection chamber was designed. The design was specialized to detect the low-energy beta ray by reducing the gap between the plastic scintillators and remove the worthless space in the detection chamber. It was confirmed how multi-channel design increase the detection efficiency through calculation using MCNP. Considering the volume of the tritiated gas in the gaps of the scintillator, expected counting rate was obtained. Through this, it was possible to design a detection chamber with maximum theoretical performance. However, it was not theoretically the maximum due to a practical problem in processing, but the optimum detection chamber was manufactured. Using the manufactured detection chamber and the electrolysis used in the chapter 3, detection efficiency was estimated. It showed much higher detection efficiency comparing with the preliminary single-channel detection chamber. The signal acceptance conditions such as gain and LDL, were optimized by defining the FOM as a parameter. The optimized signal acceptance condition is used for the final system, developed in the next chapter.

Chapter 5. Integration of the Electrolysis and Detection System

5.1 Introduction to the Real-time Continuous Tritiated Water Monitoring System

Proton exchange membrane (PEM) cells generate hydrogen gas through the electrolysis of water [53]. The PEM cell-based electrolysis is catalyst based, with a polymer membrane playing the role of the electrolyte. Because there is no need to add an additional electrolyte, it is environmentally friendly and reusable. Using PEM cells to monitor tritium in water offers two advantages. One is reduction of the self-absorption effect by gasification. The detection efficiency of tritium in water is very low because the scintillator emits beta rays with extremely low energy less than 18.6 keV and the beta ray has short range in the water. The other is the minimization of radionuclide disturbance caused by contaminants, as it undergoes a purification process before entering the PEM cell, and hydrogen gas is generated in the PEM cell; thus, the possibility of radionuclide interference problem is very low. Therefore, in the aspect of long-term operation, PEM cell-based electrolysis is suitable for continuous monitoring.

Electrolysis condition obtained in the chapter 3 and multi-channel plastic scintillator detection chamber designed and manufactured in the chapter 4 were utilized and integrated in this final chapter. The final system was designed by combining these and continuous measurement capability was tested using diluted tritiated water sample. Concentrations of the tritiated water samples were measured using liquid scintillation counter (LSC). The optimized minimum detectable activity (MDA) was calculated and effectiveness of this system was evaluated.

5.2 Calculating Concentration from Measured Counting Rate

For the purpose the developed system to monitoring tritium in water, the concentration of tritium in water sample should be displayed by calculating from the counting rate. It is reverse calculation of deriving detection efficiency (ε) as presented in Eq. (4.2). After estimating the detection efficiency, it was used as a constant to deriving tritium concentration in water. Additionally, the concentration of tritium in water sample (T_{liquid}) is determined by hydrogen volume correction factor (κ) and fractionation factor (β) as presented in Eq. (3.2). Therefore, T_{liquid} is calculated by following equation:

$$T_{liquid}\left[\frac{kBq}{L}\right] = \frac{\left(\frac{C_S}{T_S} - \frac{C_B}{T_B}\right)\cdot\kappa\cdot\beta}{\varepsilon\cdot M} \times \frac{1}{1000} \tag{5.1}$$

where C_S, C_B and M are counts of present measurement interval in sample measurement time T_S, background counts in measurement time T_B and volume of the detection chamber in L. The uncertainty of T_{liquid} is expressed as presented in Eq. (5.2):

$$\sigma^2_{T_{liquid}} = \sigma^2_\varepsilon + \sigma^2_\beta + \sigma^2_{C_B} \tag{5.2}$$

$$\sigma^2_\varepsilon = \sigma^2_{CR} + \sigma^2_\beta + \sigma^2_E + \sigma^2_V \tag{5.3}$$

where E and V are enrichment factor and volume of the water sample after electrolysis. Note that the σ_ε in (5.3) was derived in independent experiment for estimation of detection efficiency. As the electrolysis condition for estimation of detection efficiency and the continuous monitoring are same, σ_β in both equations was same. If the measurement condition is static measurement, such as measurements of sample and blank were independently conducted or peak analysis during gamma ray spectroscopy, the uncertainty would be calculated for each measurement. Applying for those cases, the uncertainty of background counting rate (σ_{C_B}) in Eq. (5.2) should be changed by uncertainty of net

counting rate ($\sigma_{C_{CR}}$). However, the developed system is a continuous monitor, and it displays a derived concentration of the tritium in water. In normal operation, because the counting rate is close to the background level, the net counting rate is very small, thus the relative error would be extremely large. Therefore, to prevent this, the relative error of T_{liquid} is expressed as a constant as a characteristic detection error in the system, which is not related to the current measured counting rate.

5.3 MDA calculation

The concept of MDA is based on the statistical hypothesis testing for decision making on presence of radioactivity. To discriminate the sample of low radioactivity and background, two types of errors are considered: false positive and false negative. The false positive error (Type I error) occurs when it is incorrectly stated the radioactivity is present though there is no radioactivity. The criterion for causing the Type I error to occur less than the desired probability (α) is called the critical level (L_C). The false negative error (Type II error) occurs when it is incorrectly state that there is no radioactivity in a sample though the radioactivity is present. This means that the error caused when net counts were recorded under the L_C though the radioactivity is present. To avoid this error, detection limit (L_D) is defined above the L_C to decrease the occurrence of Type II error less than the desired probability (β).

The net count is calculated by subtracting background counts from the gross counts. Then the net count is normally distributed with mean value of 0 if there is no radioactivity. The standard deviation of this distribution (σ_0), is obtained by propagating two standard deviations of the blank (σ_{blnak}) and the background sample (σ_B). The standard deviation of the distribution is expressed as Eq. (5.4).

$$\sigma_0 = \sqrt{\sigma_{blank}^2 + \sigma_B^2} \tag{5.4}$$

The standard deviations of blank and background is assumed as equal. The L_C is determined from this distribution, then the L_C is expressed as Eq. (5.5):

$$L_C = k_\alpha \sigma_0 \tag{5.5}$$

where k_α is the value of standard normal deviate to one-tailed probability level of 1-α. As the α is set by 0.05 in common practice, the corresponding value of k_α is 1.645. Thus, the L_C can be expressed as $2.33\sigma_B$. The L_D should be positioned above the L_C to reject the case that the counts are lower than L_C

with probability of β. When the net count of the sample is equal to L_D, the LD and the standard deviation of it (σ_D) can be expressed as Eq. (5.6) and Eq. (5.7):

$$L_D = L_C + k_\beta \sigma_D \tag{5.6}$$

$$\sigma_D = \sqrt{L_D + \sigma_0^2} \tag{5.7}$$

As the β is set by 0.05 in common practice, and σ_D is substituted into the Eq. (5.6), LD is expressed as Eq. (5.8).

$$L_D = 2.71 + 4.65\sigma_D = 2.71 + 4.65\sqrt{B} \tag{5.8}$$

L_D is a value obtained based on counting statistics and its unit is “count”. In order to convert this into a unit of radioactivity or concentration, the detection time (t) and volume (M) are divided as shown in Eq. (5.9). Additionally, the detection efficiency (ε) is divided to convert the counting rate to disintegration per time.

$$\mathrm{MDA}_{gas}\left[\frac{\mathrm{Bq}}{\mathrm{L}}\right] = \frac{\mathrm{L_D}}{\mathrm{t}\times\mathrm{M}\times\varepsilon} = \frac{2.71+4.65\sqrt{\mathrm{B}}}{\mathrm{t}\times\mathrm{M}\times\varepsilon} \tag{5.9}$$

Even though the generated gas flows into the detection chamber, the measurement inside the detection chamber can be considered static. When a sample of a certain concentration is electrolyzed and flowed to the detector, the amount of radioactivity present in the chamber is the same regardless of the flow rate. Therefore, the MDA for gaseous tritium measurement (MDA_{gas}) is expressed Eq. (5.9).

If the measurement interval is very short or the concentration of the sample changes rapidly, the detection method can be similar with the situation of scanning, and then, the MDA should be differently considered. However, in the current system, the flow rate of gas generated by electrolysis is not enough to replaces the gas in the chamber within a few seconds. And because the pretreatment before

electrolysis is required, the concentration in the sample container would not be changed rapidly. Therefore, the detecting condition is assumed as static.

The MDA_{liquid} is a system performance indicator that how low tritium concentration can be detected by this system. In case of the MDA applied for tritium in water detection(MDA_{liquid}), κ and β are further considered as presented in Eq (5.10):

$$MDA_{liquid}\left[\frac{Bq}{L}\right] = MDA_{gas}\left[\frac{Bq}{L}\right] \times \frac{\kappa \times \beta}{1000} = \frac{2.71 + 4.65\sqrt{B}}{t \times M \times \varepsilon} \times \frac{\kappa \times \beta}{1000} \quad (5.10)$$

5.4 Experimental setup

Fig. 5-1 shows a conceptual diagram of the overall developed system. The water sample is collected by using a pump. The collected sample is then filtered by using a deionization filter before being stored in a water sample tank. A peristaltic pump is used to transport the deionized water to the PEM-based electrolysis cell. Then, the remaining water and oxygen generated after the electrolysis are resupplied to the water tank. The water sample tank has the oxygen exhaust line. Next, the produced hydrogen gas is transported to the tritium detector chamber through the water trap. The water trap then removes the overflowing water and the moisture in the hydrogen gas. Finally, the measured data is recorded as spectrum data using MCA. The major difference between preliminary system and the final system is sample feeding system including pump and D.I. filter, and purge line using nitrogen gas. Additionally, drainage lines and valves are equipped for convenient experiment and completion of the system.

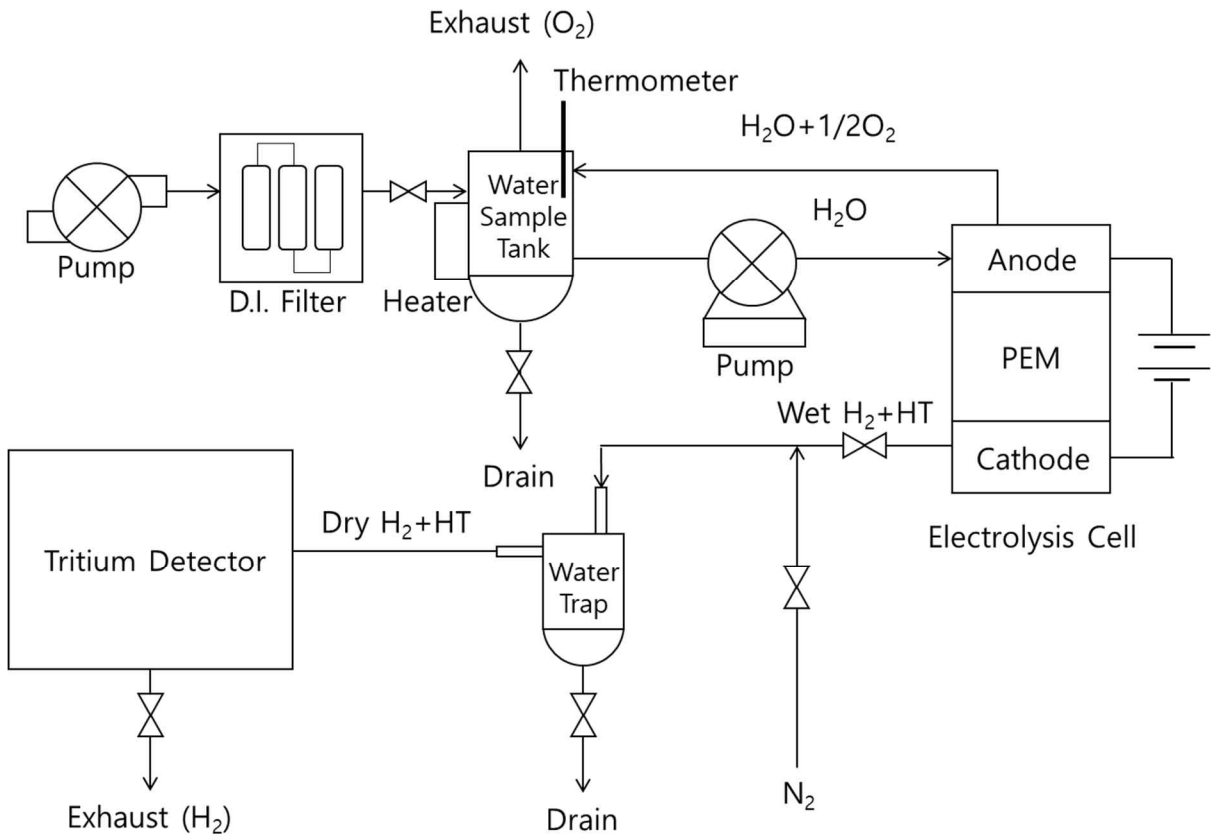

Fig. 5-1. A diagram of developed real-time on-line continuous tritiated water monitoring system

For the continuous measurement test, tritiated water sample with two different concentrations were prepared. Table 1 shows the parameters used to calculate the concentration of the electrolyzed tritiated gas. The initial volume of the tritiated water was 250 mL. The final volume of the sample is not precisely measured because a part of sample remained in the flow pipes and electrolysis cell. Because the fractionation factor at temperature of 30 ℃ was estimated by 8.90±0.38, it was utilized to calculate the expected gaseous tritium concentration. The enrichment rate was 1.07±0.05. Volume correction factor was 1240.7 assuming standard ambient temperature and pressure.

Table 5-1. Experimental parameters used to continuous monitoring of tritiated water

Parameter	Value
Initial volume (mL)	250
Final volume (calculated) (mL)	229±5
Fractionation factor	8.90±0.38
Enrichment rate	1.07±0.05
Volume correction factor	1240.7
Hydrogen flow rate (L/min)	0.49
Supplied current (A)	7.0
Volume of the detection chamber	0.424

Table 5-2 shows the concentration of the tritiated water samples. Liquid tritium concentration of the tritiated water samples were measured using LSC (Quantulus 1220, Perkin Elmer). The LSC was calibrated using certified tritium standard source. Self-made 9 vials with spiking of standard tritium source were measured with external quench parameter (SQP(E)). Using these, calibration curve was obtained with quadratic fitting.

Table 5-2. Concentration of the tritiated water samples

Sample ID	Liquid Tritium Concentration (Bq/mL)		Expected Gaseous Tritium Concentration (kBq/m^3)	
	Initial	Final	Initial	Final
T1	406.63 ± 4.14	439.6 ± 21.6	36.82 ± 1.62	39.81 ± 2.59
T2	683.12 ± 5.62	738.4 ± 35.9	61.86 ± 2.69	66.87 ± 4.33

The continuous measurement test was conducted as following step.

① Deionized water is injected to the water sample tank and electrolyzed for 30 min.

② The tritiated water sample is injected to the water sample tank after draining the deionized water. The tritiated water sample was electrolyzed for 90 min.

③ Turn off the power supply for the electrolysis cell and drain out the tritiated water sample.

④ Nitrogen gas is injected for 30 min through the purge line to clean up the remained hydrogen gases in the detection chamber.

⑤ Cleanup the water sample tank using deionized water for 5 times. Electrolysis is kept during the cleaning up. The deionized water is electrolyzed for an additional 50 minutes.

*Measurement time was 5 min. For the same sample, measurements were performed continuously.

The tritiated water sample was directly injected to the water sample tank because huge volume of tritiated water sample is required to operate the pump and pass through the D.I. filter. In this study, the experiment focused on the electrolysis and detection part to evaluate pure detection performance. The impact on detection by systemic factors will be covered in the Results and Discussion section.

5.5 Results and Discussion

Using the Eq. (4.2), the detection efficiency was estimated by 18.8 ± 2.4%. Based on this detection efficiency, the concentration of tritiated water sample was calculated using the Eq. (5.1). Fig. 5-2 and 5-3 present the continuous tritium monitoring test using tritiated water samples T1 and T2. In the T1 test initial background counting rate was 60.71 ± 0.49. After starting the electrolysis of tritiated water sample, about 30 min was required as evolving time. The maximum and average concentration in the tritiated water phase were 556 and 459 ± 85 kBq/L, respectively. During the nitrogen purge, the calculated concentration is drastically decreased even under 0 due to decrease of counting rate. The final background counting rate was 59.65 ± 0.45 cps which is slightly lower than the initial. In the T2 test as Fig. 5-3 presents, the initial background counting rate was 58.63 ± 0.33 cps. The maximum and average concentration in the tritiated water phase were 875 and 737 ± 66 kBq/L, respectively. The final background counting rate was 58.29 ± 0.59 cps. It was also slightly lower than the initial.

The volume of the hydrogen of the water trap was 1.3 L and the volume of the detection chamber was 0.424. Including the volume of the pipes, total volume of the hydrogen flow line was about 2 L. In consideration of filling the volume about 5 times when cleaning the flow path or chamber, and the hydrogen production rate of 0.49 L/min, at least 20 minutes were required to push out the existing gas and fill the produced gas in the flow path. However, it may not be effective to push a nitrogen gas filled in the detection chamber using relatively lighter hydrogen gas without sufficient pressure applied, and this may result in a difference in background counting rate after nitrogen purge. If a design is added, such as using a pressurized container to transport the generated hydrogen, the measurement can be performed more effectively.

The concentrations of the tritiated water sample were 439.6 ± 21.6 and 738.4 ± 35.9 kBq/L. Because the counting rate data in the back-end part of the tritiated water phase were used, it was reasonable to compare with the concentration of the tritiated water after electrolysis. The average values of calculated concentration were match into the 1-σ range of concentration of the tritiated water sample.

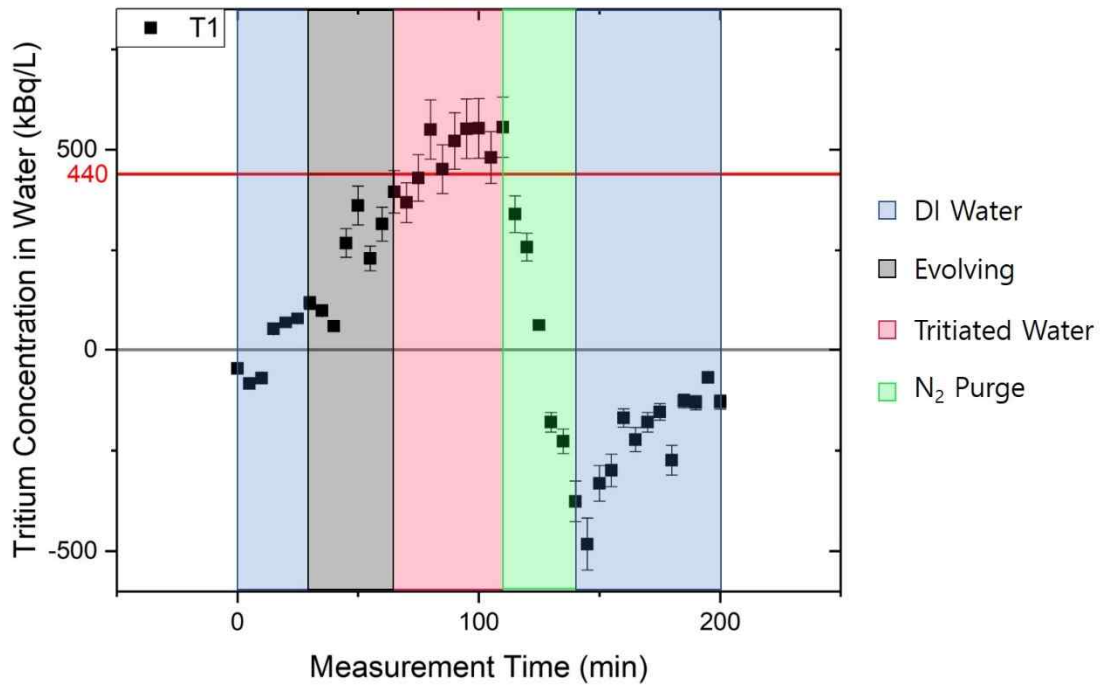

Fig. 5-2. Continuous tritium monitoring test using tritiated water sample T1

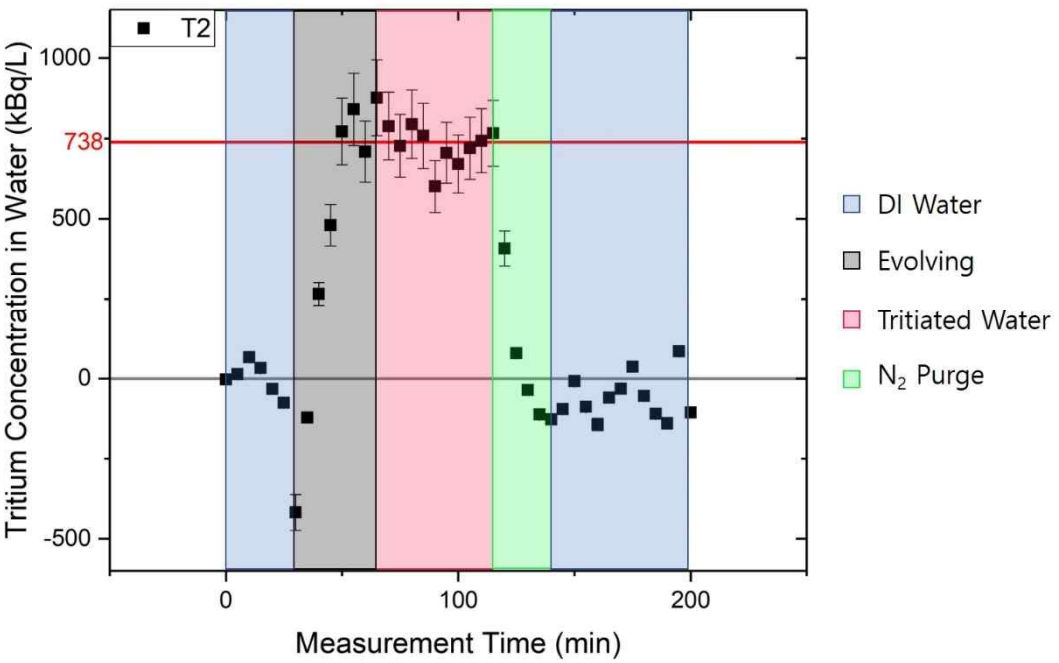

Fig. 5-3. Continuous tritium monitoring test using tritiated water sample T2

Some data points were fluctuated because of counting statistics, enrichment, and volume of the water trap vessel. The counting statistical errors inevitably occur in measurement of radiation because radioactive decay is probabilistic process. During the electrolysis, tritium in the water sample is enriched. In this process, there is difference between initial and final concentration of the tritiated water sample, the concentration of the generated gas increased. Finally, the generated gas is mixed with the occupied gas. For this reason, it takes time for the concentration of the currently electrolyzed sample to be reflected in the gas concentration in the detection chamber. This could be improved by increasing the flow rate or by using a pressurized container as mentioned above.

Fig. 5-4 shows the estimated MDA of the tritium detector for tritiated water at various temperatures of the tritiated water. The fractionation factors obtained from chapter III and detection efficiency obtained from chapter IV was used. Thus, the MDA_{liquid} shown in Fig. 5-4 implies ideally established experimental condition which used separately obtained parameters in chapter 3 and 4.

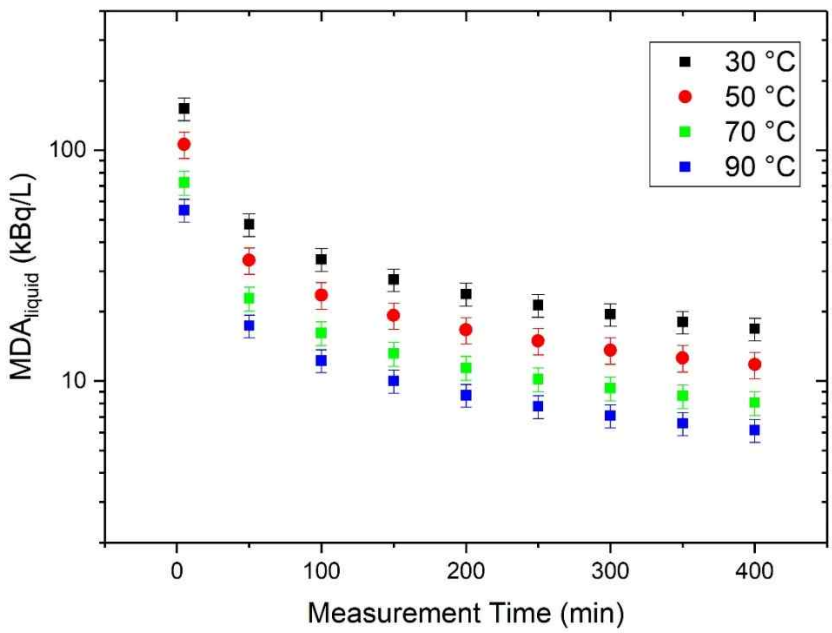

Fig. 5-4. Estimated MDAs of the tritium detection system for tritiated water for various temperatures

MDA_{liquid} was determined by the fractionation factor as presented in Eq. (3.2). When the temperature of the tritiated water increased, the MDA_{liquid} was lowered because the fractionation decreased as characterized in part I. The fractionation factor of temperature of 30 ℃ is 2.7 times higher than that of 90 ℃, and it leads to 2.7 times increase in MDA_{liquid}. Measurement time of 150 min and temperature of the tritiated water of 90 ℃ was required to satisfy the guidelines for drinking water (10 kBq/L) management published by World Health Organization [54, 55]. The MDA_{gas} for the same conditions was 2.49 ± 0.26 kBq/m^3. For the same condition but the temperature was decreased to 30 ℃, the MDA_{liquid} was 27.53 ± 3.11 kBq/L. The temperature was very dominant to determine the MDA_{liquid}, thus the temperature of the tritiated water should be monitored and maintained.

Fig. 5-5 shows the estimated MDA_{gas} and MDA_{liquid} for the developed continuous tritium monitoring system based on the test results in chapter 5 counting rate.

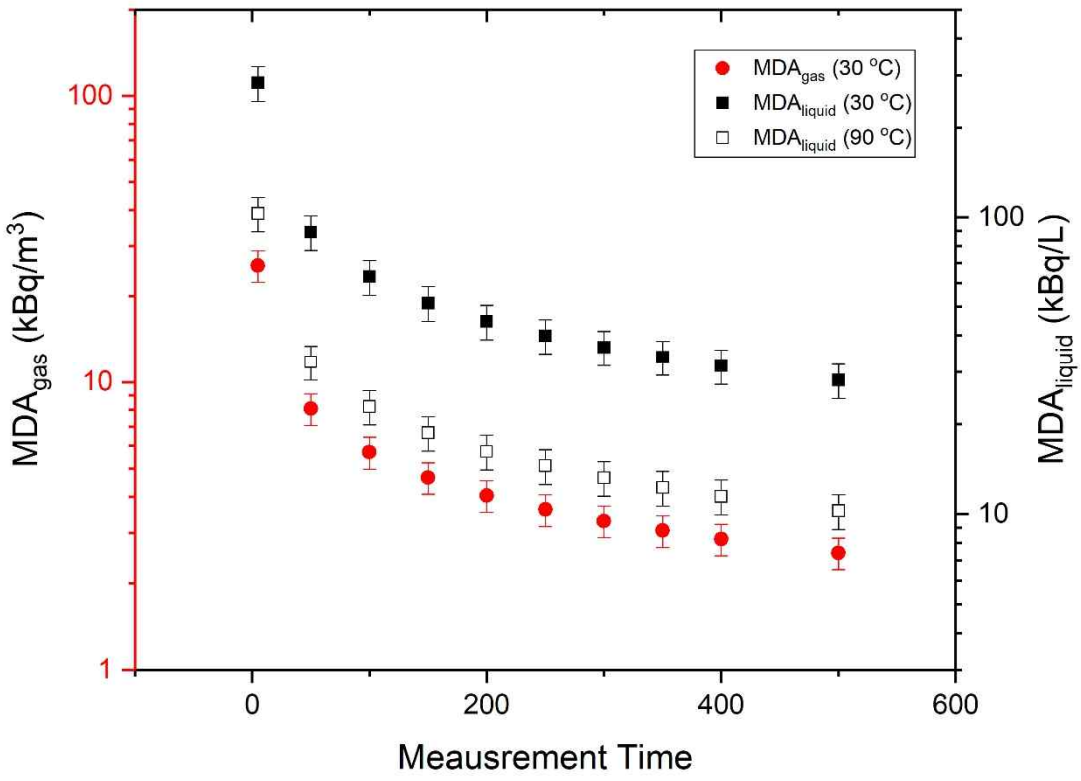

Fig. 5-5 Estimated MDAs of the tritium detection system for tritiated water for various temperatures

The MDA_{gas} and MDA_{liquid} were estimated by using Eq. (5.9) and (5.10). The MDA_{gas} was not affected by the temperature of the tritiated water sample, because it does not affect properties of the gas filled in the detection chamber. The MDA_{gas} determines how low activity of the tritiated hydrogen gas can be detected regardless of the characteristic of electrolysis.

The difference between Fig. 5-4 and Fig. 5-5 is detection efficiency and background counting rate. Different with the detector test conducted in chapter 4, detection efficiency and background counting rate were decreased. In the process of systemizing to enable continuous monitoring, there had been changes in the detection environment, such as adding a flow path and dark room conditioning. Due to changes in detection efficiency, MDA_{liquid} was increased about 87%. In the aspects of figure of merit, defined in (4.4), 3.5 times different between two experiments. It was important to optimize the detection efficiency and background counting rate to lower the MDA_{liquid}.

As an example applied to the surveying of the decommissioning site of nuclear power plants, it is recommended to have an MDA of 0.1-0.5 times the desired target concentration [56, 57]. MDA_{liquid} should be lower than 5 kBq/L to apply the developed system on the target concentration of 10 kBq/L. In this case, the measurement time of 600 min was required. The MDA_{liquid} of the developed system was lower comparing with a commercial tritium-in-water monitor, NEXGEN model has MDA of 14.8 kBq/L in 3 h, and Hofstetter's study which showed 25 kBq/L in 1 h [20]. Comparing with the Soreefan's work, it showed relatively high MDA. However, it was thought that the convenience of use was improved in terms of allowing continuous measurement and no gas consumption using a plastic scintillator instead of a proportional counter.

The developed system was sensitive to temperature. When considering commercialization, heat insulation and a precise temperature sensor and controller must be installed to precisely control the temperature of the water sample. However, this can be difficult for in-field application. In this case, there is a method of monitoring the temperature and correcting the fractionation factor in real time. When displaying the tritium concentration, a counting rate to concentration conversion coefficient as described in Eq. (5.1) is applied. The fractionation factor would be applied while changing the value based on the fitting curve. However, in this case, there is a gap between the gas in the detection chamber

being measured and the sample currently being electrolyzed. It is possible to characterize it as much as possible through flow rate, etc., but the error will still exist. The best way to operate is to go to the site, collect a certain amount of sample in a sample container, measure it completely, and move to the next sampling point. In this way, errors due to mixing among samples will be reduced and temperature control will be easy. It is also possible to continuously collect and discard samples through pumping while moving the system. In this operating condition, it is not easy to control the temperature, thus the MDA will be relatively high and unstable, therefore it is suitable to be used when a high concentration of tritium is leaked during an accident.

5.7 Summary

An on-line system for the continuous monitoring of tritium in water was developed in this chapter. The system included a PEM-based electrolysis studied in the chapter 3 and plastic scintillation chamber which was specially designed for low-energy beta ray measurement studied in the chapter 4. In the monitoring system, MDA of the target sample represents the system performance. Therefore, it was confirmed that the combined system was consistent with the analyzed results in the previous chapters, MDA_{liquid} was defined and characterized. In the 200-minute continuous monitoring test, the background and the contamination were clearly distinguishable. It has a lower MDA than commercial instruments and some past studies. Compared to some studies, it had a higher MDA, but it was considered worth taking advantage of when considering the advantages of this system. Because the system was found to be suitable as a tool to analyze large tritiated samples, it is expected that the proposed monitor can be used to perform autonomous real-time continuous tritium monitoring which does not require human intervention.

VI. Conclusion

Study on the development of tritium-in-water monitor was carried out. Because the tritium emits extremely low energy, self-absorption effect was very high, direct measurement of the liquid-state tritiated water is inefficient. Therefore, gasification using electrolysis and its specialized detector design was proposed.

Fundamental characterization of beta ray measurement using plastic scintillator was carried out. Both particle transportation simulation and essential experiment were conducted to obtain design parameters for improvement. The required thickness of the plastic scintillator was estimated by the simulation, and approximate detection efficiency was acquired. Energy spectrum of the tritium was acquired by using the plastic scintillator and energy-channel relationship was calibrated. A coincidence circuit was utilized to reject the worthless noise signals. The time difference spectrum was acquired, and its ROI was defined.

The electrolysis for the tritiated water using PEM and Pt/Ir electrode was characterized. The fractionation factor was evaluated by a method different from the previous method, which had a lower relative error compared to previous studies. Concentrations of the tritiated gas generated by the electrolysis with different concentrations of tritiated water was estimated to be linear. A preliminary tritium detector was utilized to measure the tritiated gas. Because the preliminary detector had low detection efficiency, high concentration of tritiated water sample was used, and possibility of continuous measurement was confirmed.

A plastic scintillator-based detection chamber was developed which is specialized to measure low-energy beta ray. To reduce the gap between the scintillator, which is dead-zone for the beta ray measurement, multiple scintillators were parallelly placed with short gap. Therefore, it was called multi-channel detection chamber. The design and performance test were carried out using particle transportation simulation. To gain a maximum performance, which corresponds to the lowest MDA, detection efficiency must be maximized as well as the volume of the tritiated gas in the detection

chamber. Therefore, both were considered and expected counting rate was evaluated. The optimal detection chamber design was obtained, however, because of practical problem in manufacturing, it is manufactured to have the maximum performance at the level that can be processed. Using the manufactured detection chamber was connected to the electrolysis system, its signal processing parameters such as LDL and gain was optimized.

Finally, the electrolysis and detection chamber are integrated, tritiated water sample was monitored. In the continuous monitoring test, the between counting rates background and the tritiated water were clearly distinguishable. The MDA of the system was estimated, and it had low MDA to be applied on the decommissioning site if the tritiated water long-term continuously monitored. This system is valuable in that it does not require manpower after installation and can be continuously monitored which is important to reduce the cost of decommissioning during site remediation and overall process. Additionally, it is a useful system that integrates pretreatment and measurement because it can fundamentally reject disturbances caused by other nuclides through electrolysis. it can contribute to the radiological protection of workers when used for monitoring inside the decommissioning site or NPPs in operation.

The limitation of the study in the characterization of the electrolysis is indirect measurement was used. An ionization chamber-based commercial detector for tritiated gas was used. Though it was used after being well calibrated in the laboratory, the relative error in the estimation of the fractionation factor may increase due to errors in the process of calibration. However, this error is expected to be sufficiently smaller than the error in volume or mass measurement resulting from evaporation or measurement device. Improvement of the scintillator chamber would result in improving performance of the system. The use of thinner plastic scintillator could lead to mechanical instability as well as increment of the cost. If 0.5 mm plastic scintillators are used, it is essential to place more scintillators in the chamber. To achieve this, it is needed to find a substitute material other than the acrylic. Acrylic was chosen not only for its easy processing, but also because its optical properties are similar to those of plastic scintillators, thereby reducing optical losses. If more suitable materials are found and processing methods are developed, higher performance detection chambers can be developed.

Bibliography

[1] C. Arcanjo *et al.*, "Tritiated water exposure disrupts myofibril structure and induces mis-regulation of eye opacity and DNA repair genes in zebrafish early life stages," (in English), *Aquat Toxicol,* vol. 200, pp. 114-126, Jul 2018, doi: 10.1016/j.aquatox.2018.04.012.

[2] Y. H. Choi, K. M. Lim, W. Y. Lee, S. Diabate, and S. Strack, "Tissue free water tritium and organically bound tritium in the rice plant acutely exposed to atmospheric HTO vapor under semi-outdoor conditions," (in English), *Journal of Environmental Radioactivity,* vol. 58, no. 1, pp. 67-85, 2002, doi: Doi 10.1016/S0265-931x(01)00024-8.

[3] Y. Zhang, S. Ye, and J. Wu, "A modified global model for predicting the tritium distribution in precipitation, 1960-2005," *Hydrological Processes,* Article vol. 25, no. 15, pp. 2379-2392, 2011, doi: 10.1002/hyp.8001.

[4] H. Morishima, H. Kawai, T. Koga, and T. Niwa, "The Trends of Global Tritium Precipitations," *Journal of Radiation Research,* Article vol. 26, no. 3, pp. 283-312, 1985, doi: 10.1269/jrr.26.283.

[5] J. S. Chae and G. Kim, "Dispersion and removal characteristics of tritium originated from nuclear power plants in the atmosphere," (in English), *Journal of Environmental Radioactivity,* vol. 192, pp. 524-531, Dec 2018, doi: 10.1016/j.jenvrad.2018.08.007.

[6] J. S. Chae *et al.*, "Distribution of Tritium in Water Vapour and Precipitation around Wolsung Nuclear Power Plant," (in English), *Radiat Prot Dosim,* vol. 146, no. 1-3, pp. 330-333, Jul 2011, doi: 10.1093/rpd/ncr182.

[7] R. Querfeld *et al.*, "Radionuclides in surface waters around the damaged Fukushima Daiichi NPP one month after the accident: Evidence of significant tritium release into the environment," (in English), *Sci Total Environ,* vol. 689, pp. 451-456, Nov 1 2019, doi: 10.1016/j.scitotenv.2019.06.362.

[8] H. Ohuchi, Y. Kondo, Y. Asakura, and T. Kawano, "Tritium Measurement in High Gamma-Ray

Radiation Fields by Using an Imaging Plate," (in English), *Fusion Science and Technology,* vol. 60, no. 3, pp. 944-947, Oct 2011, doi: Doi 10.13182/Fst11-A12571.

[9] Z. Grahek, B. Breznik, I. Stojković, I. Coha, J. Nikolov, and N. Todorović, "Measurement of tritium in the Sava and Danube Rivers," *Journal of Environmental Radioactivity,* Article vol. 162-163, pp. 56-67, 2016, doi: 10.1016/j.jenvrad.2016.05.014.

[10] J. Nikolov, N. Todorovic, M. Jankovic, M. Vostinar, I. Bikit, and M. Veskovic, "Different methods for tritium determination in surface water by LSC," *Applied Radiation and Isotopes,* vol. 71, no. 1, pp. 51-56, 2013/01/01/ 2013, doi: https://doi.org/10.1016/j.apradiso.2012.09.015.

[11] M. Dalla Palma *et al.*, "Pulse Shape Discrimination in Polysiloxane-Based Liquid Scintillator," (in English), *Ieee Transactions on Nuclear Science,* vol. 63, no. 3, pp. 1608-1615, Jun 2016, doi: 10.1109/Tns.2016.2530307.

[12] E. Furuta, Y. Kato, and S. Fujisawa, "Measurement of tritium with plastic scintillators in large vials of a low background liquid scintillation counter: an organic waste-less method," (in English), *J Radioanal Nucl Ch,* vol. 314, no. 2, pp. 701-708, Nov 2017, doi: 10.1007/s10967-017-5408-6.

[13] C. D. R. Azevedo *et al.*, "TRITIUM - A Real-Time Tritium Monitor System for Water Quality Surveillance," in *2018 IEEE Nuclear Science Symposium and Medical Imaging Conference, NSS/MIC 2018 - Proceedings*, 2018, doi: 10.1109/NSSMIC.2018.8824700. [Online]. Available: https://www.scopus.com/inward/record.uri?eid=2-s2.0-85073097025&doi=10.1109%2fNSSMIC.2018.8824700&partnerID=40&md5=65082e756eaed6cbda64ff72338c3f5e

[14] L. Miramonti, "A plastic scintillator detector for beta particles," *Radiat Meas,* Article vol. 35, no. 4, pp. 347-354, 2002, doi: 10.1016/S1350-4487(02)00051-3.

[15] S. Hong *et al.*, "Feasibility study on development of a fiber-optic dual detector to measure beta-And gamma-rays simultaneously," *Transactions of the Korean Institute of Electrical Engineers,* Article vol. 63, no. 2, pp. 284-290, 2014, doi: 10.5370/KIEE.2014.63.2.284.

[16] H. M. Park, K. H. Park, S. W. Kang, and K. S. Joo, "Feasibility of in situ beta ray measurements

in underwater environment," *Journal of Environmental Radioactivity,* Article vol. 175-176, pp. 120-125, 2017, doi: 10.1016/j.jenvrad.2017.05.008.

[17] K. W. Jang *et al.*, "Fiber-optic radiation sensor for detection of tritium," *Nuclear Instruments and Methods in Physics Research, Section A: Accelerators, Spectrometers, Detectors and Associated Equipment,* Conference Paper vol. 652, no. 1, pp. 928-931, 2011, doi: 10.1016/j.nima.2010.09.060.

[18] Z. Kollo, "A plastic scintillator-based activity monitor for tritiated water in the GBq/l range," (in English), *Nucl Instrum Meth A,* vol. 798, pp. 24-29, Oct 21 2015, doi: 10.1016/j.nima.2015.06.040.

[19] A. N. Singh, M. Ratnakaran, and K. G. Vohra, "An on-line tritium-in-water monitor," *Nuclear Instruments and Methods in Physics Research Section A: Accelerators, Spectrometers, Detectors and Associated Equipment,* Article vol. 236, no. 1, pp. 159-164, 1985, doi: 10.1016/0168-9002(85)90141-x.

[20] K. J. Hofstetter, "Continuous aqueous tritium monitoring," *Fusion Technology,* Article vol. 28, no. 3 pt 2, pp. 1527-1531, 1995, doi: 10.13182/fst95-a30629.

[21] T. Uda, T. Kawano, M. Tanaka, S. Tomatsuri, T. Ito, and K. Tatenuma, "Detection efficiency of plastic scintillator for gaseous tritium sampling and measurement system," (in English), *Fusion Eng Des,* vol. 85, no. 7-9, pp. 1474-1478, Dec 2010, doi: 10.1016/j.fusengdes.2010.04.019.

[22] T. Uda, K. Okuno, Y. Matsuda, and Y. Naruse, "High-Concentration Tritium Gas Measurement with Small Volume Ionization Chambers for Fusion Fuel Gas Monitors," (in English), *J Nucl Sci Technol,* vol. 28, no. 5, pp. 451-458, May 1991. [Online]. Available: <Go to ISI>://WOS:A1991FU77900009.

[23] A. Poirier and G. Douysset, "Influence of ambient humidity on the current delivered by air-vented ionization chambers revisited," *Physics in Medicine and Biology,* Article vol. 51, no. 19, pp. 4995-5006, 2006, Art no. 017, doi: 10.1088/0031-9155/51/19/017.

[24] Y. Sato, M. Shimizu, Y. Morishita, M. Sato, and M. Hoshina, "Experimental study of humidity effect on charge measurement of reference ionization chambers in clinical high-energy photon

beams," *Medical Physics,* Article vol. 46, no. 9, pp. 4177-4183, 2019, doi: 10.1002/mp.13665.

[25] T. Aoyama, H. Sugiura, and T. Watanabe, "Application of Air Proportional-Counters to a Tritium-in-Air Monitor," (in English), *Nucl Instrum Meth A,* vol. 254, no. 3, pp. 620-626, Mar 1 1987, doi: Doi 10.1016/0168-9002(87)90039-8.

[26] X. G. Tuo, K. L. Mu, Z. Li, and X. Y. Li, "Tritium Monitor Based on Gas-flow Proportional Counter," (in English), *J Nucl Sci Technol,* pp. 171-174, Jun 2008, doi: 10.1080/00223131.2008.10875814.

[27] E. Furuta and T. Ito, "Prototype apparatus for the measurement of tritium in expired air using plastic scintillator pellets," (in English), *Applied Radiation and Isotopes,* vol. 132, pp. 151-156, Feb 2018, doi: 10.1016/j.apradiso.2017.12.007.

[28] N. P. Kherani, "An alternative approach to tritium-in-water monitoring," *Nuclear Instruments and Methods in Physics Research, Section A: Accelerators, Spectrometers, Detectors and Associated Equipment,* Article vol. 484, no. 1-3, pp. 650-659, 2002, doi: 10.1016/S0168-9002(01)02008-3.

[29] A. M. Soreefan and T. A. DeVol, "Determination of tritium enrichment parameters of a commercially available PEM electrolyzer: a comparison with conventional enrichment electrolysis," (in English), *J Radioanal Nucl Ch,* vol. 282, no. 2, pp. 511-515, Nov 2009, doi: 10.1007/s10967-009-0256-7.

[30] A. M. Soreefan and T. A. DeVol, "Proportional counting of tritium gas generated by polymer electrolyte membrane (PEM) electrolysis," (in English), *J Radioanal Nucl Ch,* vol. 282, no. 2, pp. 517-521, Nov 2009, doi: 10.1007/s10967-009-0247-8.

[31] L. Roy, "Influence of temperature on the electrolytic separation factor of hydrogen isotopes," *Canadian Journal of Chemistry,* vol. 40, no. 7, pp. 1452-1460, 1962.

[32] H. Cember and T. E. Johnson, *Introduction to health physics*, 4th ed. New York: McGraw-Hill Medical, 2009, pp. xi, 843 p.

[33] A. Špalek, O. Dragoun, M. Ryšavý, and N. Dragounová, "Efficiency calibration of low-energy electron detectors by means of β-ray emitters," *Nuclear Instruments and Methods in Physics*

Research, Section A: Accelerators, Spectrometers, Detectors and Associated Equipment, Article vol. 438, no. 2-3, pp. 433-438, 1999, doi: 10.1016/S0168-9002(99)00875-X.

[34] J. F. Briesmeister, "MCNP-A general Monte Carlo code for neutron and photon transport," *LA-7396-M,* 1986.

[35] K. F. Eckerman and A. L. Sjoreen, *Radiological toolbox user's manual*. United States. Department of Energy, 2004.

[36] W. Plastino *et al.*, "Tritium in water electrolytic enrichment and liquid scintillation counting," (in English), *Radiat Meas,* vol. 42, no. 1, pp. 68-73, Jan 2007, doi: 10.1016/j.radmeas.2006.07.010.

[37] G. Garbarino, M. Magnoni, S. Bertino, and M. C. Losana, "Development of an electrolysis system for tritium enrichment in superficial water samples," *Radiat Prot Dosim,* Article vol. 137, no. 3-4, pp. 329-331, 2009, Art no. ncp244, doi: 10.1093/rpd/ncp244.

[38] L. I. Wassenaar, L. F. Han, T. Schiefer, G. Kainz, L. Araguas-Araguas, and P. K. Aggarwal, "A simple polymer electrolyte membrane system for enrichment of low-level tritium (3H) in environmental water samples," *Isotopes in Environmental and Health Studies,* Article vol. 54, no. 3, pp. 274-287, 2018, doi: 10.1080/10256016.2017.1403914.

[39] M. Groning *et al.*, "Increasing the performance of tritium analysis by electrolytic enrichment," (in English), *Isotopes in Environmental and Health Studies,* vol. 45, no. 2, pp. 118-125, 2009, doi: 10.1080/10256010902872042.

[40] M. M. Jankovic, D. J. Todorovic, Z. Keleman, and N. R. Miljevic, "The Measurement of Tritium in Water Samples with Electrolytic Enrichment Using Liquid Scintillation Counter," (in English), *Nucl Technol Radiat,* vol. 27, no. 3, pp. 239-246, Sep 2012, doi: Doi 10.2298/Ntrp1203239j.

[41] M. Saito, H. Imaizumi, N. Kato, Y. Ishii, and K. Saito, "Proton Hopping Mechanism in Solid Polymer Electrolysis Demonstrated by Tritium Enrichment and Electro-Osmotic Drag Measurement," (in Japanese), *Electrochemistry,* vol. 78, no. 7, pp. 597-600, Jul 2010, doi: DOI 10.5796/electrochemistry.78.597.

[42] A. Fukaya *et al.*, "Application of graft-type poly(ether ether ketone)-based polymer electrolyte membranes to electrochemical devices - Fuel cells and electrolytic enrichment of tritium," (in English), *Int J Hydrogen Energ,* vol. 43, no. 18, pp. 8927-8935, May 3 2018, doi: 10.1016/j.ijhydene.2018.03.103.

[43] M. Nishikawa, M. Enoeda, K. Kotoh, and K. Koga, "Enrichment and Volume Reduction of Tritiated-Water Using Electrolysis Cell Having Hydrogen Permeable Cathode," (in English), *J Nucl Sci Technol,* vol. 23, no. 10, pp. 905-913, Oct 1986, doi: 10.3327/jnst.23.905.

[44] T. Ohmori, H. Yamada, S. Narita, T. Mizuno, and Y. Aoki, "Enrichment of K-41 isotope in potassium formed on and in a rhenium electrode during plasma electrolysis in K2CO3/H2O and K2CO3/D2O solutions," (in English), *Journal of Applied Electrochemistry,* vol. 33, no. 7, pp. 643-646, Jul 2003, doi: Doi 10.1023/A:1024913110182.

[45] M. Saito, H. Imaizumi, N. Kato, Y. Ishii, and K. Sekiya, "Comparison between Anode Side and Cathode Side for Tritium Enrichment of Solid Polymer Electrolysis," (in Japanese), *Electrochemistry,* vol. 77, no. 5, pp. 370-372, May 2009, doi: DOI 10.5796/electrochemistry.77.370.

[46] S. Shiva Kumar and V. Himabindu, "Hydrogen production by PEM water electrolysis – A review," *Materials Science for Energy Technologies,* vol. 2, no. 3, pp. 442-454, 2019/12/01/ 2019, doi: https://doi.org/10.1016/j.mset.2019.03.002.

[47] A. Barros da S. Santos Neto and H. Lebre La Rovere, "Flexural stiffness characterization of fiber reinforced plastic (FRP) pultruded beams," *Composite Structures,* Article vol. 81, no. 2, pp. 274-282, 2007, doi: 10.1016/j.compstruct.2006.08.016.

[48] Y. Cao, J. Feng, and P. Wu, "Simultaneously Improving the toughness, flexural modulus and thermal performance of isotactic polypropylene by α-β crystalline transition and inorganic whisker reinforcement," *Polymer Engineering and Science,* Article vol. 50, no. 2, pp. 222-231, 2010, doi: 10.1002/pen.21521.

[49] S. Vargas, C. Vazquez, A. B. Gonzalo, and J. M. Pena, "A plastic fiber optic liquid level sensor," in *Second European Workshop on Optical Fibre Sensors*, 2004, vol. 5502: International

Society for Optics and Photonics, pp. 148-151.

[50] M. N. Gamito, "Solid angle sampling of disk and cylinder lights," in *Computer Graphics Forum*, 2016, vol. 35, no. 4: Wiley Online Library, pp. 25-36.

[51] M. Felderhoff, C. Weidenthaler, R. von Helmolt, and U. Eberle, "Hydrogen storage: the remaining scientific and technological challenges," (in English), *Phys Chem Chem Phys,* vol. 9, no. 21, pp. 2643-2653, Jun 7 2007, doi: 10.1039/b701563c.

[52] A. Ariharan, B. Viswanathan, and V. Nandhakumar, "Nitrogen-incorporated carbon nanotube derived from polystyrene and polypyrrole as hydrogen storage material," (in English), *Int J Hydrogen Energ,* vol. 43, no. 10, pp. 5077-5088, Mar 8 2018, doi: 10.1016/j.ijhydene.2018.01.110.

[53] F. Z. Aouali, M. Becherif, H. S. Ramadan, M. Emziane, A. Khellaf, and K. Mohammedi, "Analytical modelling and experimental validation of proton exchange membrane electrolyser for hydrogen production," (in English), *Int J Hydrogen Energ,* vol. 42, no. 2, pp. 1366-1374, Jan 12 2017, doi: 10.1016/j.ijhydene.2016.03.101.

[54] World Health Organization., *Guidelines for drinking-water quality*, 4th ed. Geneva: World Health Organization, 2011, pp. xxiii, 541 p.

[55] World Health Organization, *Water safety planning for small community water supplies : step-by-step risk management guidance for drinking-water supplies in small communities*. Geneva: World Health Organization, 2012, p. 55 pages.

[56] E. W. Abelquist, *Decommissioning health physics: A handbook for MARSSIM users* (Decommissioning Health Physics: A Handbook for MARSSIM Users). 2001, pp. 1-436.

[57] T. Alecksen and R. Whicker, "Scan MDCs for GPS-based gamma radiation surveys," *Health Physics,* Conference Paper vol. 111, no. 2, pp. S123-S132, 2016, doi: 10.1097/HP.0000000000000517.

Acknowledgement

저의 6 년간의 학위과정을 지원해주신 분들께 감사의 글을 올립니다. 미처 언급하지 못한 교수님, 박사님, 친구들이 있더라도 너그러이 용서해 주십시오.

먼저 지도교수님 김희령 교수님께 깊은 감사를 드립니다. 학부 3 학년 때부터 다양한 연구를 할 수 있게 길을 열어 주시고 지원해 주셔서 감사드립니다. 교수님 덕분에 다양한 연구를 경험할 수 있었고, 이는 학위 과정 중에 큰 도움이 되었습니다. 교수님의 가르침에 한 번 더 큰 감사를 드립니다.

학위논문의 심사위원으로 기꺼이 수락해주시고 많은 조언과 학위논문의 교정에 도움을 주신 이승준 교수님, 그리고 박재영 교수님께 감사드립니다. 저의 학위과정 1 년차부터 교류하며 방사선 계측분야의 공부와 연구에 도움을 많이 주신 홍상범 박사님, 전기분해와 관련하여 큰 도움을 주신 허필우 박사님께도 감사드립니다.

저와 연구실 생활을 같이했던 모든 분들께도 감사 인사를 드립니다. 정말 말그대로 동고동락했던 욱제형, 이젠 정말 박사가 되어버린 재식이형, 감초 같은 충위형, 재성이형, 근형이형, 최은정 선생님, 모두 감사드립니다. 항상 모든 일을 유쾌하게 만들어주는 시형이형, 함께 실험하느라 고생했던 기준이, 친동생 같은 우년이, 수식어를 몇 개를 붙여도 모자란 재훈이, 들어온 지 얼마 안 되었지만 대단한 영향력의 현민이, 잘 따라주었던 후배들 민지, 세원, 승훈, 승빈, 시아 모두 감사합니다. 태욱아... 너는 무사히 졸업하기를 바란다.

학부 때부터 같이 놀던 학야위 친구들 모두 고맙다. 항상 좋은 말 많이 해주는 현준이, 수정이, 동훈이, 동언이 모두 고맙고, 잊을 만하면 연락오는 동현이도 고맙다. 늘 잊지 않고 챙겨주는 도윤이, 현석이, 태건이, 무한이, 민수, 무재 다들 고맙다. 너네는 어떤 수식어를 붙여야 할지 너무 잘 아는데 그걸 붙이기엔 이 지면이 모자르... 아니, 아까우니까 생략하마.

항상 연락 먼저 해주는 우리 가족, 백옥주 여사님, 배성우 형님께도 깊은 감사를 드립니다. 자주 찾아 뵙지도, 연락도 안 하는 불효자를 용서하소서. 저를 새식구로 따뜻하게 맞아 주신 장모님, 처제, 그리고 하늘에 계신 장인어른께도 깊은 감사를 드립니다.

마지막으로, 어떻게 보면 학위과정 시작, 혹은 그 이전부터 함께해온 나의 동반자 김정화 박사님, 당신이 있어 학위과정을 무사히 마칠 수 있었습니다. 힘들 때는 지원해주고 즐거울 때는 늘 옆에 있어주어 감사합니다, 그리고 사랑합니다.

배준우 올림